JGR Biogeosciences

RESEARCH ARTICLE
10.1029/2024JG008619

Thermal Adaptation of Enzyme-Mediated Processes Reduces Simulated Soil CO_2 Fluxes Upon Soil Warming

Marijn Van de Broek[1,2], William J. Riley[3], Jinyun Tang[3], Serita D. Frey[4], and Michael W. I. Schmidt[1]

[1]Department of Geography, University of Zürich, Zürich, Switzerland, [2]Sustainable Agroecosystems group, Department of Environmental Systems Science, Swiss Federal Institute of Technology, ETH Zürich, Zürich, Switzerland, [3]Earth and Environmental Sciences Area, Lawrence Berkeley National Laboratory, Berkeley, CA, USA, [4]Center for Soil Biogeochemistry and Microbial Ecology, University of New Hampshire, Durham, NH, USA

Key Points:

- A crucial aspect of soil organic carbon (SOC) models is the representation of soil microbes
- Predicted soil CO_2 fluxes upon soil warming are reduced when accounting for microbial thermal adaptation
- On a centennial time scale, this thermal adaptation results in up to a factor of three lower predicted SOC loss

Supporting Information:

Supporting Information may be found in the online version of this article.

Correspondence to:

M. W. I. Schmidt,
michael.schmidt@geo.uzh.ch

Citation:

Van de Broek, M., Riley, W. J., Tang, J., Frey, S. D., & Schmidt, M. W. I. (2024). Thermal adaptation of enzyme-mediated processes reduces simulated soil CO_2 fluxes upon soil warming. *Journal of Geophysical Research: Biogeosciences*, *129*, e2024JG008619. https://doi.org/10.1029/2024JG008619

Received 20 NOV 2024
Accepted 21 NOV 2024

Abstract Understanding factors influencing carbon effluxes from soils to the atmosphere is important in a world experiencing climatic change. Two important uncertainties related to soil organic carbon (SOC) stock responses to a changing climate are (a) whether soil microbial communities acclimate or adapt to changes in soil temperature and (b) how to represent this process in SOC models. To further explore these issues, we included thermal adaptation of enzyme-mediated processes in a mechanistic SOC model (ReSOM) using the macromolecular rate theory. Thermal adaptation is defined here to encompass all potential responses of soil microbes and microbial communities following a change in temperature. To assess the effects of thermal adaptation of enzyme-mediated processes on simulated SOC losses, ReSOM was applied to data collected from a 13-year soil warming experiment. Results show that a model omitting thermal adaptation of enzyme-mediated processes substantially overestimates observed CO_2 effluxes during the initial years of soil warming. The bias against observed CO_2 effluxes was lower for models including thermal adaptation of enzyme-mediated processes. In addition, for a simulated linear 3°C soil warming over 100 years, models including thermal adaptation of enzyme-mediated processes simulated SOC losses of a factor of three smaller than models omitting this process. As thermal adaptation of microbial community characteristics is generally not included in models simulating feedback between the soil, biosphere and atmosphere, we encourage future studies to assess the potential impact that microbial adaptation has on soil carbon – climate feedback representations in models.

Plain Language Summary A major uncertainty in projecting how much soil organic carbon (SOC) will be converted to CO_2 as a consequence of climate change is related to how soil microbes may adapt to increasing soil temperatures. While this "microbial thermal adaptation" has been shown to occur in short-term lab incubation experiments, its effect on SOC cycling on a decadal timescale is not clear. To address this knowledge gap, a mechanistic SOC model was used to simulate data collected from a 13-year soil warming experiment, to assess how microbial thermal adaptation affects predicted SOC losses upon soil warming. The model results show that incorporating microbial thermal adaptation into the model led to reduced CO_2 effluxes from the soil to the atmosphere compared to the common approach of omitting this mechanism. Our results imply that projected SOC losses for the decades to come may be reduced when this mechanism is incorporated in land models. We therefore advocate for more research on the mechanisms controlling microbial thermal adaptation, and how to implement this mechanism in SOC models.

1. Introduction

Changes in global soil organic carbon (SOC) stocks in the coming decades will depend on how both carbon inputs, through primary productivity, and carbon losses, through organic carbon (OC) mineralization, are affected by global change (Kirschbaum, 2000; Melillo et al., 2011). As soils down to 3 m depth contain 2–6 times the amount of carbon present in the atmosphere (Scharlemann et al., 2014; Schuur et al., 2016), the transfer of even a small fraction of this SOC to the atmosphere in the form of CO_2, if not balanced by increasing inputs, can cause a positive carbon – climate feedback (Friedlingstein et al., 2001, 2014). There are, however, large uncertainties in the predicted direction and magnitude of changes in SOC stocks in the coming decades where terrestrial ecosystems are predicted to range from being a small source to a large sink of C (Friedlingstein et al., 2014; Jones et al., 2013; Mekonnen et al., 2018; Todd-Brown et al., 2014).

Conventional SOC models assume that the stability of SOC is mainly due to its chemical structure (Parton et al., 1987) following the humification theory, which has been challenged (Kleber & Lehmann, 2019; Lehmann & Kleber, 2015). These relatively simple conventional SOC model structures ignore many known processes affecting soil organic matter (SOM) dynamics (Bradford et al., 2016). Using emerging knowledge of SOC cycling, recently-developed models explicitly incorporate soil microbes (Grant et al., 2017; Riley et al., 2014; Wieder et al., 2014), extracellular enzymes (Schimel & Weintraub, 2003; Tang & Riley, 2015), and interactions between organic molecules and minerals (Ahrens et al., 2015, 2020; Dwivedi et al., 2017), often in combination. While these more mechanistic models can accurately simulate SOC concentrations on a regional scale (Zhang et al., 2020), other studies document that the response of these models diverges from the response of conventional models to changes in environmental variables (Abramoff et al., 2018; Sulman et al., 2018; Wieder et al., 2013, 2018). For instance, model intercomparison studies have demonstrated that this new generation of models produce divergent responses of SOC stocks to soil warming (Sulman et al., 2018; Wieder et al., 2018). One of the key elements to improve microbially-driven SOC models, and thus predictions for the future, is to advance understanding of soil warming effects on microbially-driven processes, and thereby improve their representation in soil biogeochemical models.

To address this need, multiple soil warming experiments have been initiated over the past several decades, with the majority of these experiments warming the topsoil layers by 3–5°C. In many soil warming experiments, it has been observed that soil CO_2 efflux (F_{CO_2}) increases upon initial soil warming, but falls back to pre-warming levels after 3–10 years (Jarvis & Linder, 2000; Melillo et al., 2002; Oechel et al., 2000; Rustad et al., 2001). However, for longer-term soil warming experiments the F_{CO_2} from heated plots did not return to values similar to the control plots after 13 years (Contosta et al., 2011), or showed an oscillatory behavior (Melillo et al., 2017). Two hypotheses have been put forward to explain the decreasing F_{CO_2} after multiple years of warming: substrate depletion and microbial thermal adaptation (Bradford, 2013). The substrate depletion hypothesis posits that upon soil warming, organic substrates that are readily available to soil microbes are consumed at increased rates, thereby depleting this microbial resource more rapidly than it can be replenished by new inputs. The thermal adaptation hypothesis posits that soil microbial communities adjust to increased soil temperatures, through physiological adjustments of individuals, shifts in microbial community composition, evolutionary adaptation, or a combination of these processes. This adaptation then decreases the rate of heterotrophic soil respiration per unit microbial biomass (Bradford, 2013). In the present study, the term "thermal adaptation" is used to encompass all potential microbial responses following a change in temperature, following Bradford (2013).

While the occurrence of substrate depletion upon soil warming has been confirmed experimentally (Bradford et al., 2008; Pold et al., 2017), the importance of microbial thermal adaptation in response to soil warming is a topic of debate (Bradford, 2013; Bradford et al., 2009; Hartley et al., 2009). On the one hand, multiple experimental studies have found no evidence of warming-induced microbial thermal adaptation (Hartley et al., 2007; Vicca et al., 2009; Walker et al., 2018). In addition, studies using theoretical models have shown that microbial thermal adaptation does not need to be invoked as a mechanism to explain the return of heterotrophic soil respiration to pre-warming values (Allison et al., 2010; Eliasson et al., 2005; Kirschbaum, 2004; W. Knorr et al., 2005; Sulman et al., 2018; Walker et al., 2018). However, reproducing the ephemeral response of heterotrophic soil respiration to soil warming, using a model without microbial thermal adaptation, does not prove that adaptation did not occur (Bradford, 2013). Allison et al. (2010), for example, showed that a microbially-explicit SOC model with either thermal adaptation of microbial communities or substrate depletion could theoretically reproduce the pattern of a short-term response of soil heterotrophic respiration to soil warming. Their model results were, however, not validated against observations.

In contrast, other studies did confirm the presence of microbial thermal adaptation. Natural temperature gradient studies have shown that soil microbial communities are adapted to their local temperature regime (Nottingham et al., 2019). Long-term field experiments (DeAngelis et al., 2017; Melillo et al., 2017; Rousk et al., 2012) and lab incubations where substrate depletion was prevented (Bárcenas-Moreno et al., 2009; Bradford et al., 2008, 2010; Dacal et al., 2019) have both shown microbial thermal adaptation. These results are consistent with the "compensatory hypothesis" (Bradford et al., 2019; Dacal et al., 2019), which attributes a negative relationship between microbial biomass specific respiration (R_s) and temperature to evolutionary trade-offs between the stability of the binding structure of enzymes and the rate at which they mediate metabolic activity. These evolutionary trade-offs arise from the fact that temperature selects for enzymes that have different conformational

flexibilities. At high temperatures, enzymes have a low conformational flexibility because of their greater rigidity, which is needed to maintain the binding between enzymes and substrates (i.e., high-temperature adapted enzymes). At low temperatures, in contrast, there is a selection toward enzymes with a higher conformational flexibility and thus higher reaction rates at cooler temperatures (i.e., low-temperature adapted enzymes). These evolutionary trade-offs imply that if soil temperatures increase, higher metabolic rates and thus higher heterotrophic F_{CO_2} will initially take place with the existing low temperature-adapted enzymes. However, microbes may acclimate by producing high-temperature adapted enzymes with a lower conformational flexibility, as they spend more time in a structure that favors their binding to substrates. This theory thus predicts that R_s will decrease after an initial increase upon soil warming. This thermal adaptation of enzyme-mediated processes and its emergent effects on microbial respiration are tested in the present study (see Section 2.2.5). It should be noted that the contribution of other mechanisms influencing the response of microbial respiration to enhanced temperatures (e.g., declines in substrate availability) has to date not been disentangled (Bradford et al., 2019; Dacal et al., 2019).

Studying the effect of thermal adaptation of enzyme-mediated processes on changes in SOC stocks on timescales relevant to Earth system processes is challenging. Therefore, we used a mechanistic soil biogeochemical model (ReSOM; Riley et al., 2022; Tang & Riley, 2015) to assess the importance of this process. We did so by applying the model to data collected over a period of 13 years from a long-term soil warming experiment at Harvard Forest (MA, USA) (Melillo et al., 2011). The advantage of this modeling approach is that indirect effects of soil warming on the surface F_{CO_2} associated with heterotropic respiration (F_{CO_2}) can be accounted for (e.g., substrate depletion or changes in soil moisture content). We incorporated thermal adaptation of enzyme-mediated processes into ReSOM by representing the relationships between soil temperature and enzyme activity using the macromolecular rate theory (MMRT) (Hobbs et al., 2013). We simulated scenarios for F_{CO_2} in the control and heated (+5°C) treatments with (a) no thermal adaptation of enzyme mediated processes, (b) optimum-driven thermal adaptation, and (c) enzyme rigidity thermal adaptation. The two latter scenarios were proposed by Alster et al. (2020).

We assessed how including thermal adaptation of enzyme-mediated processes affects (a) simulations of the short-term increase in F_{CO_2} upon initiation of soil warming by simulating an existing soil warming experiment, and (b) predictions of changes in the SOC stock in response to soil warming on a centennial time scale, for a hypothetical soil warming experiment. We hypothesized that incorporating thermal adaptation of enzyme-mediated processes into a process-based SOC model would lead to predictions of lower SOC losses upon soil warming.

2. Materials and Methods

2.1. Study Site

The data used in the model simulations were collected from a long-term soil warming experiment located at the Harvard Forest Long-term Ecological Research (LTER) site in the northeastern United States (Melillo et al., 2011). At the experimental site (Barre Woods; 42.48°N, 72.10°W), initiated in 2003, a 30 × 30 m plot was continuously warmed (+5°C above the ambient soil temperature) using heating cables buried at 10 cm depth spaced 20 cm apart. The ambient soil temperature is recorded at 10-min intervals in an adjacent 30 × 30 m control plot. The vegetation at the Barre Woods Soil Warming Study consists of an even-aged, mixed deciduous forest, dominated by *Quercus rubra*, *Q. velutina*, and *Acer rubrum* (Melillo et al., 2011). The soils at the site are coarse-loamy over sandy or sandy-skeletal mesic Typic Dystrudepts, with a pH of 5.2 in the organic horizon and 5.5 in the mineral soil (Melillo et al., 2011). The mean annual temperature is 8°C and mean annual precipitation is 1,180 mm, evenly distributed throughout the year. Detailed information about the research site and the experimental set-up can be found in (Frey & Melillo, 2021; Melillo et al., 2011). The measured data show that thermal adaptation of F_{CO_2} has taken place at Barre Woods, similar to another soil warming experiment at the same research site (Prospect Hill, Melillo et al., 2017), as shown in the Text S10 in Supporting Information S1.

2.2. Model Description

2.2.1. ReSOM

The ReSOM model (Reaction-network-based model of SOM and microbes; Riley et al., 2022; Tang & Riley, 2015) was used to assess the effect of thermal adaptation of enzyme-mediated processes on SOC dynamics.

ReSOM is a microbially-driven model that accounts for interactions between SOC, enzymes, minerals, and microbes to simulate SOC dynamics (Figure S13 in Supporting Information S1). Organic monomers and enzymes can adsorb onto mineral surfaces, protecting monomers from microbial uptake and preventing enzymes from catalyzing reactions. The model represents competition for monomers between microbes and minerals and competition for enzymes between polymers and minerals. These competition mechanisms are simulated using the equilibrium chemistry approximation (ECA, Tang & Riley, 2013). Depolymerization of polymers into monomers is simulated as follows:

$$F_S = \frac{E \cdot S \cdot V_{E,\max}}{k_{ES}\left(1 + \frac{S}{k_{ES}} + \frac{E}{k_{ES}} + \frac{M}{k_{ME}}\right)} \quad (1)$$

where F_S is the rate of depolymerization (gC m^{-3} day^{-1}), E is the extracellular enzyme pool (g C m^{-3}), S is the polymeric OC pool (gC m^{-3}), $V_{E,\max}$ the maximum rate of depolymerization (day^{-1}), and k is the affinity parameter (gC m^{-3}) for decomposition (k_{ES}) and sorption of enzymes to minerals (k_{ME}). Uptake of DOC by soil microbes is simulated as:

$$F_D = \frac{z \cdot B \cdot D \cdot V_{B,\mathrm{Max}}}{k_{BD}\left(1 + \frac{S}{k_{BD}} + \frac{E}{k_{BD}} + \frac{M}{k_{MD}}\right)} \quad (2)$$

where z is a scaling parameter for transport density (unitless), B the microbial biomass pool (gC m^{-3}), D is the monomeric OC pool (gC m^{-3}), and k is the affinity parameter (gC m^{-3}) for microbial uptake of DOC (k_{BD}) and sorption of monomers to minerals (k_{MD}).

Microbes are simulated using the dynamic energy budget (DEB) theory (Kooijman et al., 2008), which partitions microbial metabolism into structural maintenance, structural growth, and extracellular enzyme production. The DEB model used here includes a microbial internal reserve pool, serving as a buffer between substrate uptake and microbial cell metabolism, following Tang and Riley (2015). During each model time step, the turnover rate of the internal reserve pool determines how much energy is available for microbial metabolism. Before microbial structural growth or enzyme production take place, energy requirements for microbial maintenance need to be met. The remaining energy is subsequently used for microbial structural growth and extracellular enzyme production, which are assumed to have equal priorities. Microbial turnover is simulated as a density-dependent process, as implemented in a previous version of ReSOM (Sulman et al., 2018) following Georgiou et al. (2017).

In ReSOM, CO_2 is produced at different stages of microbial processing of SOC, with each step having a distinct substrate use efficiency (SUE). These stages are microbial uptake of substrate (SUE = 0.5), microbial growth (SUE = 0.8), and extracellular enzyme production (SUE = 0.8) (Tang & Riley, 2015). The overall carbon use efficiency (CUE) is calculated as:

$$CUE = 1 - \frac{P_{CO_2}^{\mathrm{metab}} + P_{CO_2}^{\mathrm{assim}}}{F_{mon}} \quad (3)$$

where $P_{CO_2}^{\mathrm{metab}}$ is CO_2 produced during microbial metabolism (sum of maintenance respiration and CO_2 production during growth and enzyme production; gC m^{-3} d^{-1}), $P_{CO_2}^{\mathrm{assim}}$ is CO_2 produced during monomer uptake by microbes (gC m^{-3} d^{-1}), and F_{mon} is the total flux of monomers to microbes (gC m^{-3} d^{-1}), before assimilation CO_2 losses occur. For the present study, the Matlab® version of ReSOM used in Sulman et al. (2018) was adapted as described in the following sections. For a full description of ReSOM, reference is made to Tang and Riley (2015).

2.2.2. Organic Horizon Compartment

The original version of ReSOM, as described in the previous section, was developed to simulate SOC dynamics in a mineral soil. As the experimental site at Barre Woods has an organic horizon, we added an organic horizon compartment to the ReSOM model (see Figure S14 in Supporting Information S1). The simulated organic horizon consists of mainly organic matter with a minor fraction of mineral-associated OC (ca. 6% of total OC in the organic horizon), as reported by Pold et al. (2017) for a nearby soil warming experiment. In the simulated organic

horizon, OC enters the organic horizon as either metabolic or structural litter, based on the lignin to N ratio of plant inputs (see Text S7 in Supporting Information S1). Both structural and metabolic litter are depolymerized into one monomer pool, with specific enzymes mediating this process. Monomers can be taken up by r- and K-strategists, or be adsorbed onto soil minerals, thereby protecting monomers from microbial uptake. It should be noted that in the soil compartment (as described in the previous section), only one microbial pool is simulated. Enzymes in the organic horizon can be adsorbed onto minerals, thereby preventing them from mediating the depolymerization of metabolic and structural litter. The equations governing the transformations of OC in the organic horizon are equal to the ones used in the mineral soil (see Tang & Riley, 2015).

2.2.3. Soil Moisture

As the original ReSOM model does not simulate the effect of soil moisture on microbial processing of SOC, we applied the equations derived by Yan et al. (2018):

$$f_m = \frac{K_\theta + \theta_{op}}{K_\theta + \theta}\left(\frac{\theta}{\theta_{op}}\right)^{1+a\cdot n_s} \text{ for } \theta < \theta_{op} \tag{4}$$

$$f_m = \left(\frac{\phi - \theta}{\phi - \theta_{op}}\right)^{b} \text{ for } \theta \geq \theta_{op} \tag{5}$$

2.2.4. Effect of Temperature on Process Rates

There are three categories of temperature-dependent processes in ReSOM: (a) equilibrium reactions, (b) nonequilibrium reactions, and (c) enzyme-mediated reactions (Abramoff et al., 2019; Tang & Riley, 2015). Equilibrium reactions include processes of reversible binding (monomer-mineral, enzyme-polymer, and enzyme-mineral) and microbial maintenance (Tang & Riley, 2015). The temperature dependency of the affinity parameters is simulated based on the transition state theory (Eyring, 1935):

$$K_{EQ}(T) = K(T_0)\, exp\left[-\frac{\Delta G_{EQ}}{R}\left(\frac{1}{T} - \frac{1}{T_0}\right)\right] \tag{6}$$

Where $K(T_0)$ is the reference affinity (gC), ΔG_{EQ} is the Gibbs free energy change of the equilibrium reaction (kJ mol^{-1}), R is the gas constant (J K^{-1} mol^{-1}), T is the current temperature (K) and T_0 is the reference temperature (K). Nonequilibrium and non-enzyme reactions involve the maximum rates for adsorption of monomers and enzymes, of which the temperature-dependency is calculated as (Tang & Riley, 2015):

$$V_{\mathrm{NEQ}}(T) = V(T_0)\ \frac{T}{T_0}\exp\left[-\frac{\Delta G_{\mathrm{NEQ}}}{R}\left(\frac{1}{T} - \frac{1}{T_0}\right)\right] \tag{7}$$

where $V(T_0)$ is the reference maximum rate (d^{-1}) and ΔG_{NEQ} is the Gibbs free energy change of the nonequilibrium reaction (kJ mol^{-1}). Enzyme-mediated processes include the uptake of monomers, depolymerization of polymers by extracellular enzymes, and microbial reserve turnover. In previous applications of ReSOM, the temperature-dependency of these processes was simulated based on the fraction of enzymes inactivated through reversible denaturation at a given temperature, resulting in an optimum temperature at which the fraction of active enzymes is maximal. In order to simulate thermal adaptation of enzyme-mediated processes in ReSOM according to established hypotheses (Alster et al., 2020), this formulation has been replaced with the macromolecular rate theory (Hobbs et al., 2013), as presented in Section 2.2.5.

2.2.5. Temperature Sensitivity and Thermal Adaptation of Enzyme-Mediated Processes

The temperature sensitivity of enzyme-mediated processes is implemented in ReSOM according to the macromolecular rate theory (MMRT; Hobbs et al., 2013). Specific processes leading to thermal adaptation of enzyme-mediated processes (e.g., evolutionary trade-offs between the structure and function of enzymes or changes in microbial community composition) were not identified in this study, but we simulated the combined effect of these processes on rates of enzyme-mediated processes. The MMRT accounts for declines in enzymatic activity at

temperatures below which denaturation of enzymes takes place, resulting in a unimodal relation between temperature and rates of enzymatic processes. Since biological reactions are generally mediated by macromolecules with large heat capacities (e.g., enzymes), the formulation of the MMRT renders the shape of the temperature response curve a function of the change in heat capacity between the enzyme-substrate and the enzyme-transition state complex (Hobbs et al., 2013):

$$\ln(k) = ln\left(\frac{k_b\ T}{h}\right) - \frac{\Delta H^{\ddagger}_{\boldsymbol{T_0}} + \Delta C^{\ddagger}_P (T - T_0)}{R\ T} + \frac{\Delta S^{\ddagger}_{\boldsymbol{T_0}} + \Delta C^{\ddagger}_P\ (ln(T) - Ln(T_0))}{R} \tag{8}$$

where k is the rate, k_b is the Boltzmann constant (J K^{-1}), h is Planck's constant (J s), R is the universal gas constant (kJ K^{-1} mol^{-1}), T is the temperature (K), T_0 is the reference temperature (K), $\Delta H^{\ddagger}_{T_0}$ and $\Delta S^{\ddagger}_{T_0}$ are the differences in enthalpy and entropy between the transition state and the ground state at T_0 (kJ mol^{-1} K^{-1}) and $\Delta C^{\ddagger}_P$ is the difference in heat capacity between the transition state and the ground state at constant pressure (kJ mol^{-1} K^{-1}). Negative values of $\Delta C^{\ddagger}_P$ result in a negative curvature of the temperature-rate relationship, with larger negative values resulting in a steeper and narrower curve. More detailed information about the MMRT is provided in Hobbs et al. (2013), Schipper et al. (2014), and Arcus et al. (2016).

Applying (Equation 8) results in rate values (k) between 0 and ∞. To avoid correlations between values of maximum process rates (V_{max}) and the value of k, we used the MMRT to calculate a rate modifier in the range [0–1] by dividing the calculated values of k by the value of k at the optimum temperature (see below). The rate modifier calculated using MMRT was applied to (a) the maximum DOC uptake by microbes ($V_{B,max}$), (b) the metabolic turnover rate of microbes (κ), (c) the maximum SOC degradation rate ($V_{E,max}$), and (d) the maximum rate of desorption of monomers and enzymes from soil minerals ($V_{max\_des\_mon}$ and $V_{max\_des\_enz}$). We assumed that other temperature-dependent, non-enzyme-mediated processes were not subjected to thermal adaptation.

The MMRT model has four parameters that need to be specified: T_0, $\Delta C^{\ddagger}_P$, $\Delta H^{\ddagger}_{T_0}$, and $\Delta S^{\ddagger}_{T_0}$. To limit the number of parameters to estimate, we followed the recommendation by Alster et al. (2020) to fix the value of T_0 to 4–10 K below the value of T_{opt}. As the value of T_0 does not strongly affects the model fit (Alster et al., 2016; Schipper et al., 2014), we fixed its value at 6 K below the median T_{opt} of 305.9 K found in a meta-analysis by Alster et al. (2018), resulting in a value for T_0 of 299.9 K. Furthermore, we used the strong linear relationship between $\Delta H^{\ddagger}_{T_0}$ and $\Delta S^{\ddagger}_{T_0}$ from the meta-analysis by Alster et al. (2018) to obtain that $\Delta S^{\ddagger}_{T_0} = 0.0033\,\Delta H^{\ddagger}_{T_0} - 204.01$ ($R^2 = 0.91$, data present in their supplementary data, only data obtained for soil environments were used). The value for T_{opt} can be calculated by setting the first derivative of (Equation 8) to zero, for $\Delta C^{\ddagger}_P < 0$ (Arcus et al., 2016):

$$T_{opt} = \frac{\Delta H^{\ddagger}_{\boldsymbol{T_0}} - \Delta C^{\ddagger}_P\ T_0}{-\Delta C^{\ddagger}_P - R} \tag{9}$$

To obtain a formulation of how T_{opt} varies with soil temperature in the thermal adaptation scenarios (see below), the value for T_{opt} was optimized during model calibration, while the value for $\Delta H^{\ddagger}_{\boldsymbol{T_0}}$ was calculated by re-arranging (Equation 9):

$$\Delta H^{\ddagger}_{\boldsymbol{T_0}} = T_{opt}\left(-\Delta C^{\ddagger}_P - R\right) + \Delta C^{\ddagger}_P\ T_0 \tag{10}$$

In this study, we implemented three scenarios of thermal adaptation of enzyme-mediated processes. The first scenario assumed no thermal adaptation, that is, a static MMRT curve irrespective of fluctuations in soil temperature. In the other two scenarios, the shape of the MMRT curve was a function of the average soil temperature over n days prior to the simulated day (t_{adapt}). Two hypotheses proposed by Alster et al. (2020) were applied: (a) the optimum driven scenario and (b) the enzyme rigidity driven scenario (Figure 1).

No adaptation scenario. This scenario (Figure 1a) assumes that the relationship between soil temperature and the rate of enzyme-mediated processes is independent of soil temperature fluctuations. Two parameter values need to

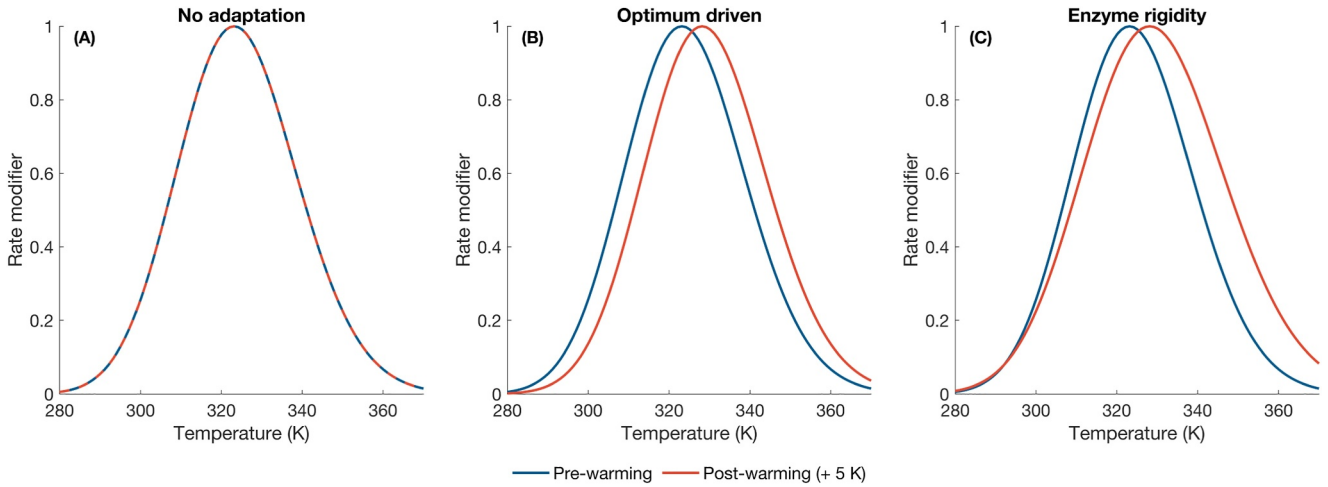

Figure 1. Relationships of rate modifiers for enzyme-mediated processes and soil temperature for the three thermal adaptation scenarios tested in this study for a situation in which the soil temperature increases by 5 K: (a) no thermal adaptation, (b) optimum driven, and (c) enzyme rigidity (with a wider curve upon soil warming).

be optimized in this scenario to obtain the relationship between temperature and the rate modifier, T_{opt} and $\Delta C_P^{\ddagger}$, which remain constant throughout the simulation.

Optimum driven scenario. In this scenario (Figure 1b), the value for T_{opt} is a function of soil temperature, with T_{opt} increasing with temperature while the value for $\Delta C_P^{\ddagger}$ remains constant. The temperature affecting T_{opt} is calculated as the mean soil temperature over a fixed number of days prior to the simulated day (t_{adapt}), with the relation between T_{opt} and the temperature during t_{adapt} (T_{avg}) being assumed to be linear:

$$T_{opt} = \alpha_T \, T_{avg} + \beta_T \tag{11}$$

with α_T being the slope (K K^{-1}) and β_T the intercept (K). The variable α_T thus represents the change in T_{opt} per K change in soil temperature. This approach results in four MMRT parameters that need to be optimized: t_{adapt}, $\Delta C_P^{\ddagger}$, α_T, and β_T.

Enzyme rigidity scenario. In this scenario (Figure 1c), an increase in soil temperature causes $\Delta C_P^{\ddagger}$ to become less negative, resulting in a wider curve, and T_{opt} to increase. The relationship between T_{opt} and T_{avg} is calculated as in (Equation 11), while the relation between $\Delta C_P^{\ddagger}$ and T_{avg} is calculated as:

$$\Delta C_P^{\ddagger} = \alpha_C \, T_{avg} + \beta_C \tag{12}$$

with α_C being the slope (kJ mol^{-1} K^{-2}) and β_C the intercept (kJ mol^{-1} K^{-1}). The variable α_C thus represents the change in $\Delta C_P^{\ddagger}$ per K change in soil temperature. This approach results in five MMRT parameters that need to be optimized: t_{adapt}, α_T, β_T, α_C, and β_C. For a mechanistic explanation about these scenarios, reference is made to Alster et al. (2020).

2.3. Data Processing

Data to drive and calibrate ReSOM were obtained from multiple sources reporting data collected from Harvard Forest, as described in detail in the Supplementary Information S1. Briefly, to calculate rate modifiers based on soil temperature and soil moisture, available data on soil and air temperature and soil moisture were obtained and processed (Boose & Gould, 2004; Frey & Melillo, 2021). Aboveground plant carbon inputs were calculated using data on annual litterfall (Finzi et al., 2019, 2021), while the temporal distribution of litterfall within the year was calculated using data on litterfall at different times during the year (Munger & Wofsy, 2021). Litterfall inputs to the organic horizon were divided into structural and metabolic carbon following Parton et al. (1987), using data from Frey and Ollinger (2021) and Magill et al. (2004). The magnitude of belowground OC inputs was obtained

using data from Finzi et al. (2020), while the temporal variability of belowground OC inputs within a year was calculated using data from Abramoff and Finzi (2016). Model parameter values were optimized by comparing modeled SOC stocks to SOC stock measurements down to 30 cm in the Barre Woods control plot in 2011 (Finzi et al., 2020) (no SOC stocks for heated treatments were reported) and F_{CO_2} measurements, which were made monthly during the growing season (April to November) every year starting in 2003 (Frey & Melillo, 2021). Measured F_{CO_2} were partitioned into autotrophic and heterotrophic respiration components based on previous calculations made at Harvard Forest (Savage et al., 2018), of which the heterotrophic F_{CO_2} was used as model calibration data. The measured total SOC stock was partitioned to be comparable to the model pools using data from DeAngelis et al. (2017), Gaudinski et al. (2000), McFarlane et al. (2013), and Pold et al. (2017). Detailed information about data processing is provided in the Sections 1.1–1.9 in Supporting Information S1.

2.4. Model Application

2.4.1. Application to Barre Woods

While there are three soil warming experiments at Harvard Forest (Contosta et al., 2011; Melillo et al., 2011, 2017), ReSOM was only applied to the experiment at Barre Woods. The reason for this choice is that this warming experiment consisted of 30 by 30 m megaplots which encompass whole trees, enabling us to account for the effect of differences in litterfall between the control and heated plots. This is not possible for the other two experiments, which consist of smaller plots (3 by 3 or 5 by 5 m). ReSOM was applied to the soil warming experiment at Barre Woods from the onset of the experiment (May 2003) until 2016, and model output was produced at a 1-day time step. The model simulated the evolution in the SOC stock in the organic horizon and the mineral soil to a depth of 0.3 m, and the resulting F_{CO_2} from these model compartments. A model spin-up was run for a period of 100 years to equilibrate the SOC content at the 2003 experiment onset. This time span was sufficient to obtain modeled SOC pools at steady state. After the spin-up was run, both the control and heated treatments were simulated independently with the same initial conditions after spin-up. Thermal adaptation was only simulated to occur for microbial enzyme-mediated processes to assess the emergent effect on SOC stocks and F_{CO_2}. To test how thermal adaptation of enzyme-mediated processes affects modeled SOC stocks and F_{CO_2}, the model was run using the three thermal adaptation scenarios (see Section 2.2.5). Thermal adaptation was implemented to occur throughout the entire simulation, including spin-up.

2.4.2. Model Calibration

The number of model parameter values that was optimized differed for the three thermal adaptation scenarios: 16 for the no thermal adaptation scenario, 18 for the optimum driven scenario, and 19 for the enzyme rigidity scenario. Parameter optimization was performed in Matlab® using a genetic algorithm. This algorithm uses concepts from evolutionary theory, such as selection, crossover, and mutation, to modify the sets of parameters tested during every iteration of the optimization procedure to optimally explore the parameter space. The genetic algorithm was run with a population size of 360 individuals (i.e., parameter sets) until the fitness value did not improve for 15 consecutive iterations. The upper and lower bounds of parameter values allowed during calibration are provided in Table S2 in Supporting Information S1.

To calculate the fitness values, the following measurements were compared to their modeled equivalent: the measured heterotrophic F_{CO_2} for the control and heated treatment separately (109 data points per treatment), the total SOC stock for the control treatment in 2011 (1 data point), and the distribution of this carbon into structural, metabolic, and mineral-associated OC for the organic horizon, and polymeric and mineral-associated OC for the soil layer. The errors for the modeled F_{CO_2} on the one hand, and SOC stocks on the other hand, were calculated separately and combined in the overall model error. The error for modeled F_{CO_2} was calculated using the Nash-Sutcliffe efficiency:

$$\varepsilon_{NS} = 1 - \frac{\sum_{i=1}^{n} \left(y_i - \hat{y}_i\right)^2}{\sum_{i=1}^{n} \left(y_i - \bar{y}\right)^2} \tag{13}$$

where y_i is the ith measurement, $\hat{y}_i$ is the ith modeled value, and $\bar{y}$ is the average of measurement i to n. As the genetic algorithm searches for the minimum error, the model error was formulated as $-\varepsilon_{NS} + 1$. This way, a

perfect fit of the model results in an error of 0, while less good fits result in positive values. In addition, to detect a systematic overunderestimation or overestimation of simulated F_{CO_2}, the mean absolute error (MAE) was calculated:

$$\mathrm{MAE} = \sum_{i=1}^{n} \frac{(\hat{y}_i - y_i)}{n}$$

The errors for organic horizon and mineral soil OC stocks was calculated as the relative root mean squared error (RRMSE):

$$\varepsilon_{\mathrm{RRMSE}} = \sqrt{\left(\frac{y - \hat{y}}{y}\right)^2} \tag{14}$$

Where y is the measured SOC stock in 2011 and $\hat{y}$ the modeled SOC stock. The overall model error ($\varepsilon_{\mathrm{tot}}$) was calculated as the sum of the individual errors (i.e., ε_{NS} and $\varepsilon_{\mathrm{RRMSE}}$, both unitless), with the errors for the F_{CO_2} given a weight twice that of the individual errors for the organic horizon and soil OC stocks, as more data on F_{CO_2} were available. We note that while microbial and enzymatic properties have been measured at other soil warming experiments at Harvard Forest (e.g., Mark A. Bradford et al., 2008; DeAngelis et al., 2015; Pold et al., 2017), it was chosen not to include these in the model evaluation data. This would involve making adaptations to the model so that it explicitly simulates the measured properties, which would mean including more model parameters that need to be calibrated. Instead, these data are used for model evaluation (see Section 4.2). The optimized models for each thermal adaptation scenario were compared using the Akaike Information Criterium (AIC):

$$\mathrm{AIC} = ln\left(\frac{\mathrm{SSR}}{N}\right) + 2n_p \tag{15}$$

where SSR is the sum of squared residuals for the measured versus modeled F_{CO_2}, N is the number of observations, and n_p is the number of calibrated model parameters.

2.4.3. Scenario Analysis

To assess the long-term effects of including thermal adaptation of enzyme-mediated processes in a SOC model, the three calibrated models were run for the three thermal adaptation scenarios for 100 years over which a linear soil warming of 3°C was imposed. This magnitude of warming was chosen as it is in the middle of the range of predicted increases in atmospheric temperature in 2100 by the IPCC (IPCC, 2023). The same model inputs were used as for the simulations of the Barre Woods site. First, the models were run for 100 years as described in Section 2.4.1 up to the same date as soil warming in Barre Woods was initiated (May 2003). Subsequently, the daily soil temperatures for the control run for the next 100 simulation years was equal to the average daily temperatures of the respective days during the period 1978–2003, the soil temperature being linearly increased by 3°C during the 100 simulation years, relative to the soil temperature of the control treatment. It is noted that OC inputs were not affected by soil warming in these projections, as the aim was to assess how the presence or absence of microbial thermal adaptation influences SOC stocks and subsequent F_{CO_2}, without other confounding factors.

3. Results

3.1. Parameter Optimization

The optimal values for the model parameters obtained using the genetic optimization algorithm are shown in Table S1. The optimization procedure found a similar total error (i.e., the sum of (i) 2 ($-\varepsilon_{NS-c}$ + 1) + 2 ($-\varepsilon_{NS-h}$ + 1) and (ii) $\varepsilon_{\mathrm{RRMSE}}$; the subscripts c and h refer to the control and heated plots, resp.) for the no thermal adaptation ($\varepsilon_{\mathrm{tot}}$ = 1.86; ε_{NS-c} = 0.62, ε_{NS-h} = 0.48, $\varepsilon_{\mathrm{RRMSE}}$ = 0.06), the optimum driven ($\varepsilon_{\mathrm{tot}}$ = 1.89; ε_{NS_c} = 0.62, ε_{NS_h} = 0.47, $\varepsilon_{\mathrm{RRMSE}}$ = 0.06) and enzyme rigidity ($\varepsilon_{\mathrm{tot}}$ = 1.84; ε_{NS_c} = 0.63, ε_{NS_h} = 0.47, $\varepsilon_{\mathrm{RRMSE}}$ = 0.02) scenarios. Despite these similar errors, simulated changes in SOC content and net CO_2 loss over

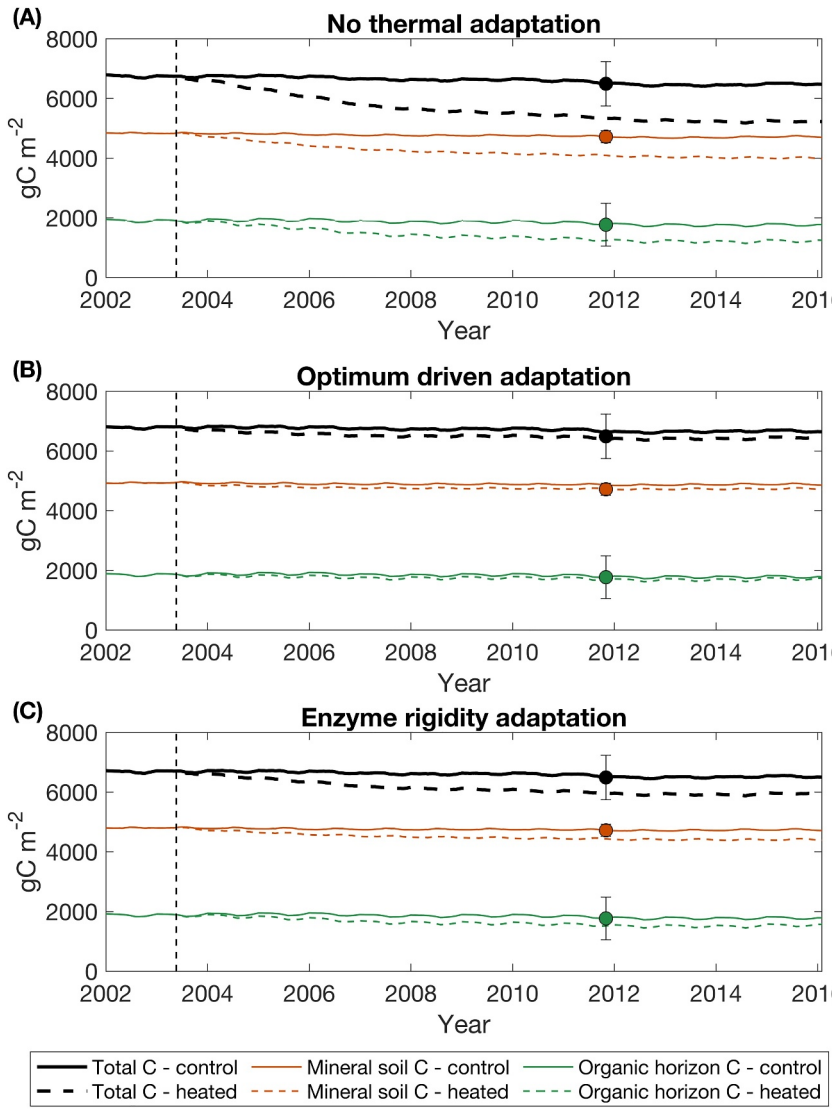

Figure 2. Simulated changes in soil organic carbon (SOC) stocks in the organic horizon (green lines), mineral horizon (brown lines) and their combination (total C, black lines) for the control treatment (solid lines) and heated treatment (dashed lines). Results are shown separately for the no thermal adaptation scenario (a), the optimum driven adaptation scenario (b), and the enzyme rigidity scenario (c). The filled circles show October 2011 measured values for the SOC stock in the control treatment for the organic horizon (green), mineral soil (brown), and their combination (black). The initiation of soil warming is indicated by the vertical dashed line.

the 13-year period differed considerably between the models including and excluding thermal adaptation, as shown in the next sections.

3.2. Simulated Changes in SOC Stocks

After parameter optimization, the measured organic horizon and mineral SOC stocks were accurately simulated for the control treatments of all three scenarios (Figure 2). However, the magnitude of the simulated change in OC in the organic horizon and mineral soil upon warming differed between the scenarios. The largest decrease in SOC upon soil warming was simulated for the no thermal adaptation scenario (−31% and −15% for the organic horizon and mineral soil, respectively), while the simulated decrease was substantially lower for the optimum driven (−4 and −3%) and the enzyme rigidity (−14% and −7%) scenarios. Including thermal adaptation of enzyme-mediated processes thus led to a substantially lower simulated decrease in SOC stocks upon warming. No measurements of

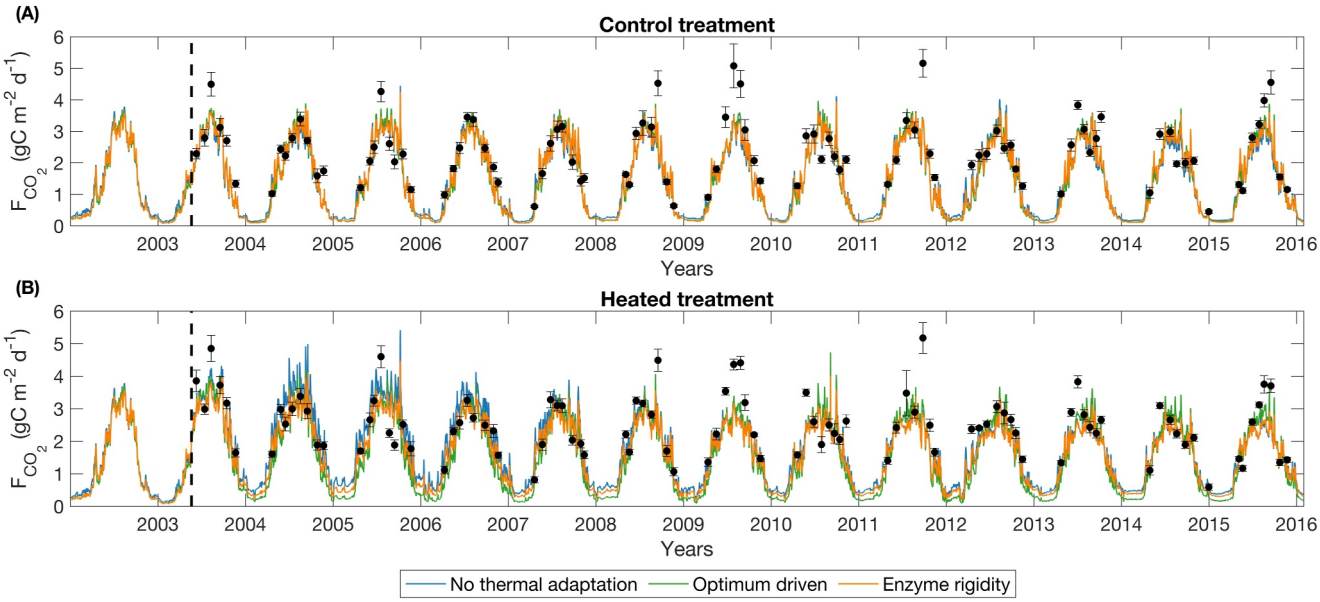

Figure 3. Daily observed and simulated surface heterotrophic CO_2 effluxes (F_{CO_2}), combined for the organic horizon and mineral soil, for the control (a) and heated (b) treatment for the three thermal adaptation scenarios. The initiation of soil warming is denoted by the vertical dashed line and black circles denote measured F_{CO_2}.

changes in SOC stocks were available for the site we simulated. However, we compare simulated and observed heterotrophic F_{CO_2} in Section 3.3.

In the organic horizon under the no thermal adaptation scenario, the relative losses from different SOC pools were largest for metabolic (−39%) and structural (−37%) litter, while losses of mineral-associated OC were substantially smaller (−4%) (Figure S15 in Supporting Information S1). It is noted that in the simulated organic horizon SOC consisted mainly of partially decomposed organic matter, with a minor fraction of mineral-associated OC (Pold et al., 2017). A similar pattern of losses was observed in the optimum driven scenario, albeit with smaller losses (−20% for metabolic litter, −12% for structural litter). In the enzyme rigidity scenario, however, losses for structural litter (−27%) were larger than losses for metabolic litter (−17%). Under both thermal adaptation scenarios, mineral-associated OC in the organic horizon slightly decreased upon soil warming (−6% and −1% in the optimum driven and enzyme rigidity scenarios, respectively).

In the mineral soil horizon, a substantial amount of polymeric OC was lost upon warming under the no thermal adaptation scenario (−31%), while the mineral-associated OC pool decreased by 3% (Figure S16 in Supporting Information S1). The optimum driven and enzyme rigidity scenarios led to small gains in mineral-associated OC (+4 and + 2% respectively), while the decrease in polymeric OC was less than under the no thermal adaptation scenario (−13% and −20% for the optimum driven and the enzyme rigidity scenarios, respectively).

3.3. Modeled Versus Measured F_{CO_2}

We calculated multiple goodness of fit measures to assess the extent to which the thermal adaptation scenarios were able to reproduce measured F_{CO_2} (Figures 3 and 5, Table S3 in Supporting Information S1). These measures were calculated separately for different time periods following the initiation of soil warming to assess model performance during the initial peak in F_{CO_2} (years 1–4), in the subsequent years (years 5–13), and in all simulated treatment years combined (years 1–13). This was done to emphasize the difference in model performance during the peak in simulated F_{CO_2}, and in subsequent years. Although the relative root mean squared errors (RRMSE) were similar for the different scenarios when calculated for all simulated treatment years (0.61–0.67 gC m^{-2} d^{-1}), there were substantial differences in the MAE and slope of the relationships between measured and modeled daily F_{CO_2}.

The MAEs calculated for all scenarios and all simulated treatment years combined were negative (Figure 5), indicating an underestimation of the simulated average daily F_{CO_2}. This overall negative MAE may indicate that

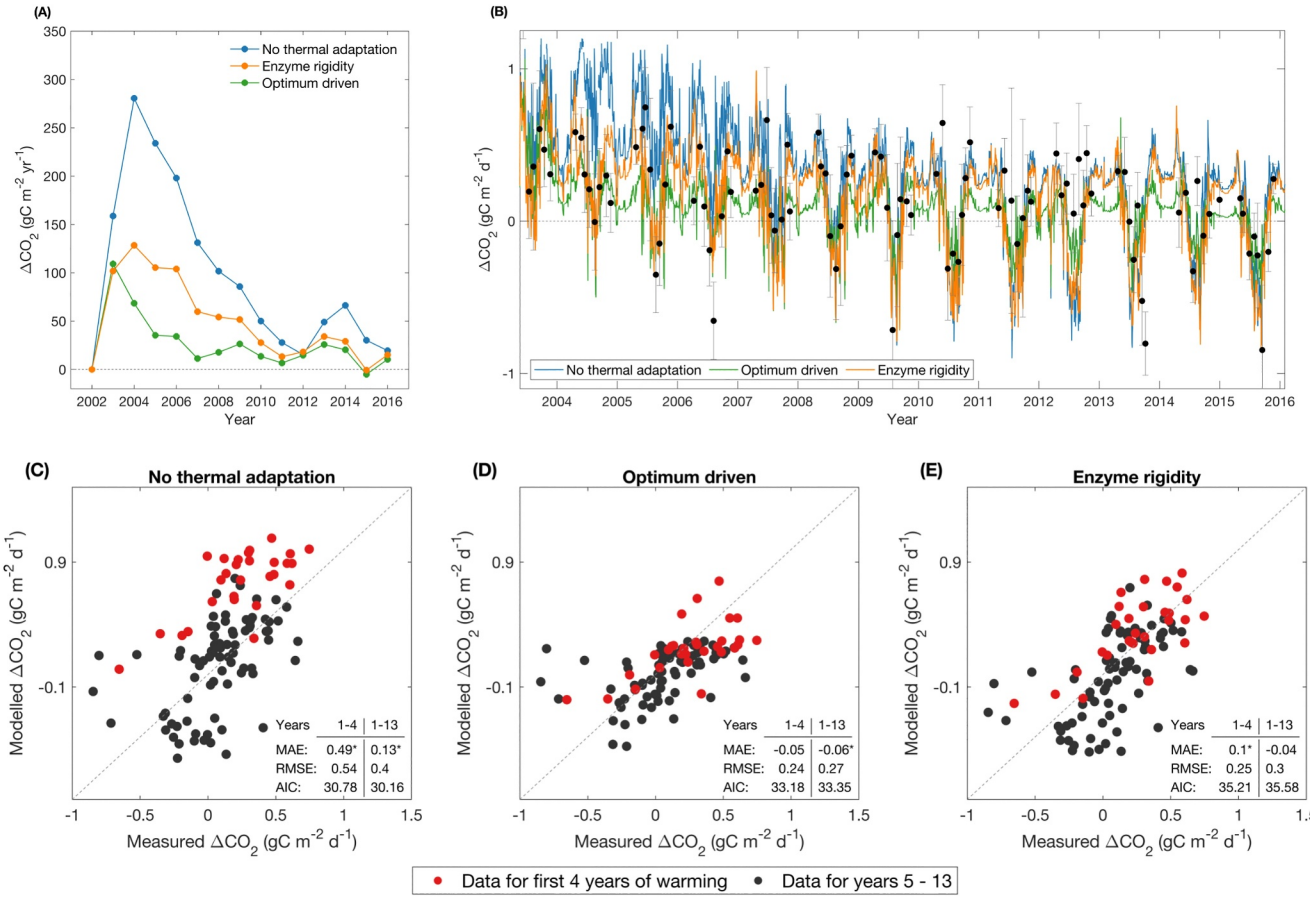

Figure 4. Difference in simulated annual (a) and daily (b) CO_2 effluxes (F_{CO_2}) between the control and heated treatment (ΔF_{CO_2}) for the three thermal adaptation scenarios, combined for the organic and mineral horizons. Positive values indicate that F_{CO_2} from the heated treatment were larger than from the control treatment. Black dots in (b) indicate measured ΔF_{CO_2}, no data for observed annual differences is available. (c–e) Show measured versus modeled ΔF_{CO_2} for the different scenarios, with red dots indicating data for the first 4 years upon the initiation of warming. The units of mean absolute error (MAE) and RMSE are gC m^{-2} d^{-1}. MAE values with an * are significantly different from 0.

the simulated OC inputs to the soil were underestimated. However, the MAE during the first 4 years of soil warming for the no thermal adaptation scenario was positive and substantially larger (0.18 gC m^{-2} d^{-1}) compared to both thermal adaptation scenarios (−0.34 and −0.20 gC m^{-2} d^{-1}). This difference was also apparent when calculating the difference between annual F_{CO_2} in the heated and control treatment (ΔF_{CO_2}; gC m^{-2} yr^{-1}) (Figure 4a). The peak in ΔF_{CO_2} after the initiation of soil warming was lowest for the optimum driven scenario (ca. 110 gC m^{-2} yr^{-1}), followed by the enzyme rigidity scenario (ca. 130 g C m^{-2} yr^{-1}) and the no thermal adaptation scenario (280 gC m^{-2} yr^{-1}). Although no measured data on the annual ΔF_{CO_2} was available, the positive simulated annual ΔF_{CO_2} bias for the no thermal adaptation scenario during the first 4 years after soil warming (Figure 5d) suggests that this scenario overestimates measured daily F_{CO_2}.

This overestimation is also apparent when comparing measured daily ΔF_{CO_2} values with modeled values for the no thermal adaptation scenario (blue line in Figure 4b). The no thermal adaptation scenario thus significantly overestimates measurements, with a MAE of 0.49 gC m^{-2} d^{-1} during the initial 4 years of warming (Figure 4c). This MAE is much lower for both thermal adaptation scenarios (−0.05 to 0.1 gC m^{-2} d^{-1}; Figures 4d and 4e). While the model simulations thus generally underestimate the F_{CO_2}, the underestimation for both the control and heated treatment by the thermal adaptation scenarios leads to a simulated ΔF_{CO_2} consistent with measurements (Figures 4d and 4e), while the no thermal adaptation scenario overestimates the response of the F_{CO_2} to soil warming (Figure 4c). The simulated cumulative amount of CO_2 lost from the heated treatments relative to the control treatment over 13 years of soil warming was substantially larger for the no thermal adaptation scenario

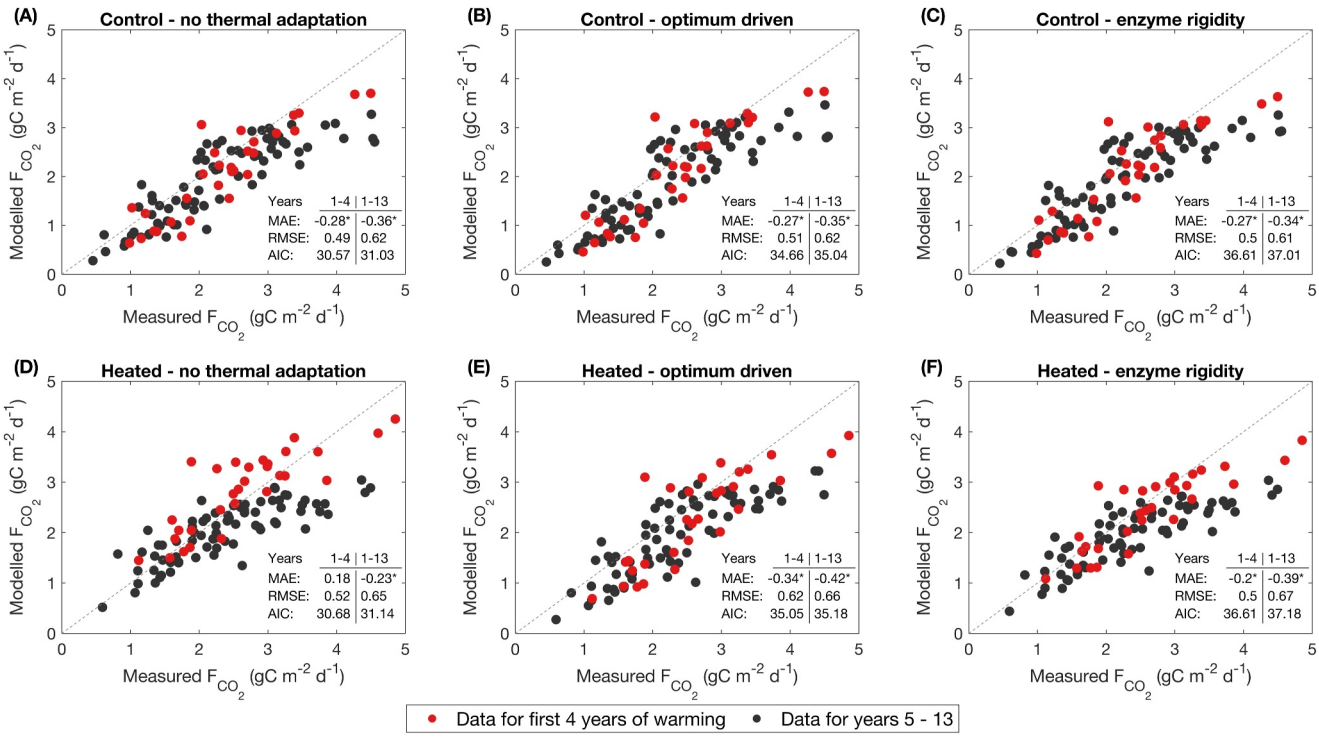

Figure 5. Simulated versus measured daily CO_2 effluxes (F_{CO_2}), combined for the organic and soil horizons, for the control (a–c) and heated treatment (d–f) and the three thermal adaptation scenarios. Red symbols show F_{CO_2} during the first 4 years after initiation of soil warming, while black symbols show the fluxes in years 5–13. The gray dotted lines are the 1:1 lines, error measures are reported on the graphs and in Table S3 in Supporting Information S1. The units of mean absolute error (MAE) and RMSE are gC m^{-2} d^{-1}. MAE values with an * are significantly different from 0.

(ca. 1,450 gC m^{-2}) compared to the thermal adaptation scenarios (ca. 390 and 730 gC m^{-2} for the optimum driven and enzyme rigidity scenarios, respectively) (Figure S18 in Supporting Information S1).

To compare the performance of the three model scenarios while accounting for model complexity, the AIC was calculated for both modeled F_{CO_2} (Figure 5), and the daily simulated ΔF_{CO_2} (Figures 4c–4e). For both measures, and for all time periods considered, the AIC was in the order of no adaptation < optimum driven < enzyme rigidity. This suggests that the added complexity, in the form of additional model parameters to simulate thermal adaptation, leads to overparameterization compared to the no thermal adaptation scenario. It should, however, be noted that the calculation of AIC only accounts for the sum of squared residuals, a measure for the difference in modeled versus measured values which does not account for a systematic overunderestimation or overestimation of simulated F_{CO_2} (Equation 15). This lack of accounting for the systematic bias is an important shortcoming for the results presented here, as all models have a similar error (see Section 3.1) while it is the consistent overestimation of F_{CO_2} predictions under soil warming without thermal adaptation that leads that an overestimation of the additional amount of CO_2 produced under warming compared to the control (Figure 4c).

3.4. Differences in MMRT Parameters for the Different Scenarios

The optimized model parameters to calculate the MMRT rate modifiers are shown in Table S4 in Supporting Information S1, while the resulting MMRT curves pre-warming (1998–2000) and post-warming (2010–2012) are shown in Figure S25 in Supporting Information S1. In the no thermal adaptation scenario, the shape of the MMRT curve was independent of soil temperature (Figure S25A in Supporting Information S1), leading to the same positive relationship between soil temperature and maximum enzyme reaction rates irrespective of soil temperature. The situation was different in both thermal adaptation scenarios. In the optimum driven scenario (Figure S25B in Supporting Information S1), for every degree increase in soil temperature, the value for T_{opt} increased by 0.65 K, causing lower maximum rates at the same temperature compared to before soil warming. In the enzyme rigidity scenario, T_{opt} increased by 0.86 K and $\Delta C_P^{\ddagger}$ increased by 0.34 kJ mol^{-1} K^{-1} per degree of average soil

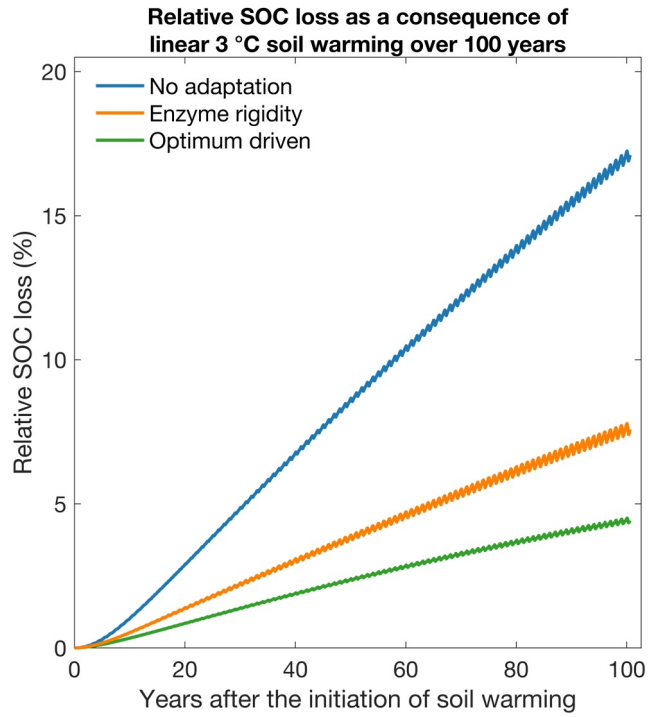

Figure 6. Simulated relative loss of soil organic carbon (SOC) under linear soil warming of 3°C over 100 years using three thermal adaptation scenarios: no thermal adaptation, enzyme rigidity, and optimum driven thermal adaptation. The optimized model parameter values obtained in this study were used. The model was applied to data collected from the Barre Woods Soil Warming Study at Harvard Forest, starting with the control steady state SOC pools at the beginning of the warming experiment (2003). Note that C inputs to the system were held constant and were the same for all three scenarios.

warming. As in the optimum driven scenario, the change in the shape of the MMRT curve led to lower maximum reaction rates at a given temperature after soil warming (Figure S25C in Supporting Information S1). For both thermal adaptation scenarios, a variable was optimized to determine the time prior to the simulated day over which the average temperature determines the value of T_{opt} and $\Delta C_P^{\ddagger}$ (t_{adapt}). These values were 345 d and 365 d for the optimum driven and enzyme rigidity scenarios, respectively, showing that it took about 1 year for the rates of enzyme-mediated processes to adapt to elevated soil temperatures in the model simulations (Figure S19 in Supporting Information S1).

3.5. Effect of Thermal Adaptation for a Gradual Centennial Increase in Soil Temperature

The model simulated substantially different SOC losses between the no thermal adaptation and the two thermal adaptation scenarios when imposing a 3°C linear increase in soil temperature over 100 years (Figure 6). When expressed relative to the amount of SOC before soil warming started, the no thermal adaptation scenario resulted in a SOC loss of ca. 17%, while both thermal adaptation scenarios led to lower simulated losses of 4.5% and 7.5%. We note that SOC inputs where not affected by soil warming in these projections.

4. Discussion

4.1. Simulation of the Ephemeral Character of the Soil CO_2 Efflux in Response to Soil Warming

The +5°C soil warming at the Barre Woods Soil Warming Study caused an increase in heterotrophic F_{CO_2} during the initial years following soil warming (Melillo et al., 2011, Text S10 in Supporting Information S1). Our results show that over the 13-year period, the models including thermal adaptation simulated a warming-induced increase in the soil heterotrophic CO_2 flux (F_{CO_2}) 50%–73% lower compared to the model where thermal adaptation was omitted (Figures 4 and S18 in Supporting Information S1). This lower F_{CO_2} resulted in a lower loss of available substrate in the soil (ca. 31% for the no thermal adaptation scenario vs. 13% and 20% losses for the optimum driven and enzyme rigidity scenarios, respectively). In addition to thermal adaptation of enzyme-

mediated processes, substrate depletion also contributed to the decrease in F_{CO_2} over time. As a real-world soil experiment was simulated, our model set-up did not allow for the evaluation of a baseline scenario (i.e., a scenario without substrate depletion). It is therefore not possible to quantify the relative contribution of both mechanisms (thermal adaptation vs. substrate depletion) to the decrease in F_{CO_2} over time. However, our results show that in the absence of thermal adaptation of enzyme-mediated processes (with substrate depletion being the only mechanism), the increase in F_{CO_2} in the heated treatment compared to the control, and thus SOC losses, are overestimated during the initial years of soil warming (Figure 4). This result is in line with evidence of both substrate depletion and thermal adaptation jointly contributing to an ephemeral increase in F_{CO_2} in response to soil warming (Bradford et al., 2008; Li et al., 2019). Our model results are thus in line with previous findings that microbial thermal adaptation is at least partly, but not solely, responsible for the decreasing F_{CO_2} over time with soil warming, together with a loss in available substrate.

4.2. Comparison With Previous Research at Harvard Forest

The comparison of the model results with data for which direct observations were available for the Barre Woods Soil Warming Study (i.e., heterotrophic F_{CO_2}) showed that the models including thermal adaptation performed better during the initial years following the initiation of soil warming compared to the model omitting this process. To assess if the simulation of other model pools is in line with observations, data collected from two other +5°C soil warming experiments at Harvard Forest were used: the Soil Warming x Nitrogen Addition Study (Contosta et al., 2011) and the Prospect Hill Soil Warming Study (Melillo et al., 2017). The analysis presented in this section allows an indirect assessment of model performance, which is used here to provide research directions for further model development.

The simulated SOC losses due to soil warming differed between the no thermal adaptation scenario and the scenarios including thermal adaptation (Table 1). Measurement-inferred losses using a CO_2 mass balance approach have shown that in comparison to the control plot, heated soils lost 11.3% SOC (after 10 years, down to 30 cm depth; Melillo et al., 2002), 15% SOC (after 7 years of warming, down to 60 cm depth; Melillo et al., 2011), 23% (after 16 years, down to 20 cm; (M. A. Knorr et al., 2024) and 17% (after 26 years, down to 60 cm depth; Melillo et al., 2017) across the three soil warming experiments at Harvard Forest. These observationally-constrained estimates suggest that the no thermal adaptation scenario (−19.4%) is at the high end of reported SOC losses, while both thermal adaptation scenarios underestimated SOC losses (−3.4% to −8.8%). It is noted that quantifying changes in SOC stocks upon soil warming is very challenging, as Melillo et al. (2017) did not detect changes in SOC stocks using soil samples at the Prospect Hill Soil Warming Study, while Finzi et al. (2020) calculated that 103 soil samples would be necessary to detect a significant change in SOC stocks at this experiment. In addition, calculating changes in SOC stocks from CO_2 mass balance approaches is challenging, given uncertainties due to, for example, difficulties to separate the F_{CO_2} into heterotrophic and autotrophic respiration, and the high number of measurements needed to reliably calculate annual F_{CO_2} from individual measurements. It is therefore challenging to make a direct comparison between simulated and measured changes in SOC stocks for the simulated experiment.

In a previous modeling study simulating coupled plant-soil carbon and nitrogen dynamics at the Barre Woods experiment, Grant (2014) simulated a SOC loss of 786 g C m^{-2} for the initial 7 years of the experiment. Simulated SOC losses with ReSOM for the no thermal adaptation scenario are higher than this model results (a loss of ca. 1,150 g C m^{-2} during the initial 7 years), while the average simulated SOC loss for the thermal adaptation scenarios combined for this time period (ca. 450 g C m^{-2}) is lower.

Concerning changes in the amount of mineral-associated OC upon soil warming, the model omitting thermal adaptation simulated a small decrease (−3.5%), while the models including thermal adaptation simulated a small increase (2.4%–3.9%; Table 1). The results for all models are consistent with the observational study of Liu et al. (2021), who found no significant effect of +5 K soil warming on the amount of mineral-associated OC in micro and macroaggregates after 27 years of soil warming at Prospect Hill. However, Pold et al. (2017) reported an observed decrease in the amount of mineral-associated OC of 45% after ca. 24 years of soil warming at Prospect Hill. Drawing conclusions about model performance in terms of the effect of soil warming on changes in the amount on mineral-associated OC is thus difficult, given the large range in reported data.

Table 1
Comparison Between Selected Variables Simulated in This Study and Reported in Previous Studies

Variable	This study			Previous studies
	No thermal adaptation	Optimum driven	Enzyme rigidity	
ΔSOC[a]	−19.4%	−3.4%	−8.8%	−11.3%[i]
				−15%[j]
				−17%[k]
				−23%[l]
$\Delta MAOC$[b]	−3.5%	+3.9%	+2.4%	−45%[m]
				No effect[n]
ΔMBC_{org}[c]	+6.3%	−10.0%	+1.1%	−31.7%[g]
				−29.9%[e]
ΔMBC_{min}[d]	+3.7%	+10.0%	−4.2%	−20.9%[o]
				−21.7%[m]
				−45%[l]
ΔDOC_{org}[e]	−29.3%	+2.6%	−20.7%	−19%[o]
ΔDOC_{min}[f]	−26.6%	−26.9%	−14.5%	−30%[o]
$CUE_{control}$[g]	0.31	0.31	0.33	0.25–0.50[n]
				0.42 (0.25–0.67)[q]
				0.15–0.18[l]
CUE_{heated}[h]	0.29	0.27	0.30	0.25–0.50[n]
				0.39 (0.19–0.66)[q]
				0.10[l]

Note. Variables that report a simulated quantitative change are calculated as the difference for the last 3 years of soil warming between the control and heated treatment. The results from the present study are presented separately for the three thermal adaptation scenarios. [a]Relative change in SOC stocks, combined for the organic horizon and mineral soil. [b]Relative change in the amount of mineral-associated OC. [c]Relative change in microbial biomass carbon in the organic horizon. [d]Relative change in microbial biomass carbon in the mineral soil. [e]Relative change in the amount of OC available to microbes in the organic horizon. [f]Relative change in the amount of OC available to microbes in the mineral soil. [g]CUE in the mineral soil for the last 3 years of the control treatment. [h]CUE in the mineral soil for the last 3 years of the heated treatment. [i]Melillo et al. (2002). [j]Melillo et al. (2011). [k]Melillo et al. (2017). [l]M. A. Knorr et al. (2024). [m]Pold et al. (2017). [n]Liu et al. (2021). [o]Bradford et al. (2008). [p]Frey et al. (2008). [q]Li et al. (2018).

With respect to changes in the amount of microbial biomass carbon due to soil warming, ReSOM simulated changes between −10.0% and +10.0% for the different scenarios in the organic and mineral soil horizons (Table 1). In contrast, studies have consistently reported a decrease in the amount of microbial biomass carbon for the +5°C soil warming experiments at Harvard Forest in the range of −20% to −45% (Bradford et al., 2008; Frey et al., 2008; Pold et al., 2017). In a study conducted at the Prospect Hill warming experiment at Harvard Forest, Pold et al. (2017) found that 24 years of +5°C soil warming led to an increase in extracellular enzyme activity per unit microbial biomass of 30%–78%, while microbial biomass decreased because the supply of substrate could not keep up with microbial demand. Although the current version of ReSOM simulated an increase in the activity of extracellular enzymes with warming, it failed to simulate a decrease in labile OC availability under the thermal adaptation scenarios (see next paragraph). The latter may have caused overestimation of microbial biomass with warming. In addition, in the current version of ReSOM, the microbial turnover rate is independent of soil temperature, although turnover rates have been shown to increase with warming (Hagerty et al., 2014). This issue may also have contributed to the overestimation of microbial biomass upon soil warming. More work is thus needed to include the temperature sensitivity of additional processes (such as microbial turnover rate) to improve model simulations.

The model results showed that after 11–13 years of warming, the average simulated amount of substrate available to microbes, relative to the control treatment, was lower under the no thermal adaptation scenario (−27.9% for the organic horizon and soil combined) compared to the thermal adaptation scenarios (−12.2% for the optimum driven scenario, −17.6% for the enzyme rigidity scenario) (Table 1, Figure S21 in Supporting Information S1).

When comparing these results to Bradford et al. (2008), who reported an average decrease in DOC of 19% and of mineralizable OC of 30% in the organic horizon and mineral topsoil combined at Prospect Hill, it seems that the model omitting thermal adaptation better simulates the dynamics of available OC upon soil warming, while the model including thermal adaptation underestimate its decrease. A potential reason is the higher calibrated depolymerization rates in the no thermal adaptation scenario, compared to both thermal adaptation scenarios (Table S1 in Supporting Information S1). While the reason for this behaviour is unclear, it seems that the lower amounts of DOC simulated by the no thermal adaptation scenario led to the overestimation of F_{CO_2}. As no observations of DOC content for the simulated experiment (i.e., Barre Woods) were available, changes in the size of this pool could not be accounted for during model calibration. To simulate the dynamics of internal model pools reliably, in addition to correctly simulating the overall behaviour of the system, data on simulated model pools are thus necessary (Sierra et al., 2015).

The average CUEs simulated during the last three years (years 11–13) for the soil under the no adaptation scenario (0.29–0.31) were similar to the CUEs in thermal adaptation scenarios (0.27–0.33) (Table 1, Figure S22 in Supporting Information S1). These values are in between measurements made by (M. A. Knorr et al., 2024) at the Soil Warming x Nitrogen Addition Study (between 0.10 and 0.18), and by Liu et al. (2021) for microbes in micro- and macroaggregates at Prospect Hill (between ca. 0.25 and 0.50). In addition, in a study simulating soil warming at the Prospect Hill soil warming experiment in Harvard Forest using the MEND model, Li et al. (2018) obtained CUEs of 0.42 for the control treatments and of 0.39 for the heated treatment. While these values are ca. 0.1 higher than the values that emerged from ReSOM, the relative difference in CUE between the control and heated treatments was similar. The CUE values emerging in ReSOM are thus consistent with values obtained in previous empirical studies, but different from previous modelling studies. The commonly used measure to quantify microbial thermal adaptation in soils is mass specific respiration (R_s) (i.e., the amount of CO_2 produced per unit microbial biomass (Bradford et al., 2008, 2019; Dacal et al., 2019)). For the simulated soil layer during the last three simulation years, R_s increased by 12.7% under the no thermal adaptation scenario in the heated compared to the control treatment, decreased by 7.0% under the optimum driven scenario, and increased by 19.5% under the enzyme rigidity scenario. This simulated decline in R_s with soil warming for the optimum driven scenario is consistent with results from soil incubation experiments along climate gradients (Bradford et al., 2019; Dacal et al., 2019). However, while Bradford et al. (2008) reported a decrease in R_s with soil warming at Harvard Forest, this decrease was attributed to a decrease in microbial biomass and respiration in the heated soils. This result is contradictory to our simulated increase in microbial biomass with soil warming under the optimum driven scenario. It thus seems that while the model predicts the correct response for the optimum driven scenario, that is, a decrease in R_s with soil warming, the mechanisms causing this effect, that is, microbial biomass and CUE rsponses to soil warming, need to be improved.

In summary, while the models including thermal adaptation reproduce measurements of the F_{CO_2} well during the initial years of soil warming, more work is needed to improve simulations of the effect of increasing temperatures on the dynamics of multiple model pools, such as mineral-associated OC, microbial-available OC, and soil microbes.

4.3. Considerations for Future Research Related to the Simulation of Thermal Adaptation of Enzyme-Mediated Processes

While results from lab incubation experiments with samples collected along climatic gradients (Bradford et al., 2019; Dacal et al., 2019) and long-term soil warming experiments (Bradford et al., 2008; Guo et al., 2020) have shown that soil microbes adapt to changing thermal regimes, there are large uncertainties about how to include this process in microbially explicit SOC models (Alster et al., 2020). In the present study, the macromolecular rate theory (sensu Hobbs et al., 2013) was used to simulate the relationship between soil temperature and enzyme activity. Alternatively, other relationships, such as the square root (Ratkowsky) model (Bååth, 2018; Ratkowsky et al., 1982), which requires fewer parameters to be calibrated, or the Chemical Kinetics Theory (Tang & Riley, 2024) can be tested for their potential to simulate this process. Our simulations show that models including thermal adaptation of enzyme-mediated processes outperform a model omitting this process in terms of simulating the response of heterotrophic soil respiration to soil warming during the initial years of soil warming. However, as we did not explicitly simulate the processes responsible for thermal adaptation, future studies should explore if including these mechanisms in SOC models improves simulation results. For example, microbial thermal adaptation, in the broad sense as used in this study, has been attributed to changes in microbial community composition and function upon soil warming (Bradford, 2013; Guo et al., 2020; Morrison et al., 2019), a process that has been

observed in multiple soil warming experiments (DeAngelis et al., 2015; Frey et al., 2008; Guo et al., 2020; Pold et al., 2015, 2016; Zhou et al., 2012) and combined lab incubation and field studies (Oliverio et al., 2017). Given the difficulties in teasing apart mechanisms contributing to microbial thermal adaptation in soils, SOC models simulating the effect of biotic and abiotic factors on the microbial community composition (e.g., Allison, 2012; Brzostek et al., 2014) can be used to explore the extent to which this process contributes to microbial thermal adaptation. Further research should then assess whether including this process in SOM models improves predictions, given the trade-off between model complexity and data availability.

In the present study, the SOC cycle was simulated without accounting for interactions with soil nutrients or the biosphere. This is an important caveat, as soil warming has a large effect on ecosystem properties affecting the SOC cycle (Grant, 2014). For example, soil warming can affect the rate of both above (Butler et al., 2012; Melillo et al., 2002, 2011) and belowground (Arndal et al., 2018; Melillo et al., 2011; Song et al., 2019; WU et al., 2011) OC inputs to the soil, along with nitrogen mineralization (Butler et al., 2012; Contosta et al., 2011; Melillo et al., 2002, 2011; Zhou et al., 2012). In this study, we accounted for changes in aboveground net primary productivity due to soil warming, but assumed the annual rate of belowground OC inputs to be constant and equal in the simulated control and heated treatments, due to the absence of data on this process. As changes in OC inputs have a large effect on heterotrophic soil respiration, incorporating microbial thermal adaptation in ecosystem models is a necessary next step to quantify the effect this process has on changing SOC stocks in the ongoing warming world.

5. Conclusions

Our results show that SOC models including thermal adaptation of enzyme-mediated processes simulate a substantially lower soil CO_2 efflux upon warming compared to a model omitting this process during the initial years following a +5°C soil warming at Harvard Forest. This distinction was mostly evident from a substantial positive MAE of simulated differences in soil CO_2 production between the heated and control treatments upon warming by the model without thermal adaptation. Models including thermal adaptation of enzyme-mediated processes simulated cumulative CO_2 losses over the course of the 13-year soil warming experiment to be 50%–73% lower compared to a model omitting thermal adaptation. Using a scenario in which soil temperature increases linearly by 3°C on a centennial timescale, including thermal adaptation of enzyme-mediated processes, reduced projected SOC losses by up to a factor of ca. three compared to a model omitting thermal adaptation. Given the limited research of this mechanism in real-world experiments to date, but the potentially large implications for the simulation of SOC changes with soil warming, we encourage further research into this topic to increase confidence in model simulations of future SOC stocks.

Conflict of Interest

The authors declare no conflicts of interest relevant to this study.

Data Availability Statement

Software for this research (ReSOM codes with the necessary data for model calibration) is available at: Van de Broek and Tang (2024).

Acknowledgments
We are thankful to Kathleen Savage and Rose Abramoff for sharing data from their work at Harvard Forest. We further thank Mel Knorr for providing data from the Harvard Forest data archive and for her help with data formatting. This work was supported by the U.S. Department of Energy Office of Science, Office of Biological and Environmental Research Terrestrial Ecosystem Science Program under award DE-SC-0001234 to Lawrence Berkeley National Laboratory for the Belowground Biogeochemistry Scientific Focus Area, and by the Swiss National Science Foundation (SNF) within project 172744 (DEEP C). The Barre Woods Soil Warming Study was maintained with support from the U.S. National Science Foundation LTER Program (DEB-1832110) and a Long-Term Research in Environmental Biology grant (DEB-1456610) to SDF.

References

Abramoff, R. Z., & Finzi, A. C. (2016). Seasonality and partitioning of root allocation to rhizosphere soils in a midlatitude forest. *Ecosphere*, *7*(11), 1–20. https://doi.org/10.1002/ecs2.1547

Abramoff, R. Z., Torn, M. S., Georgiou, K., Tang, J., & Riley, W. J. (2019). Soil organic matter temperature sensitivity cannot be directly inferred from spatial gradients. *Global Biogeochemical Cycles*, *33*(6), 761–776. https://doi.org/10.1029/2018GB006001

Abramoff, R. Z., Xu, X., Hartman, M., O'Brien, S., Feng, W., Davidson, E., et al. (2018). The millennial model: In search of measurable pools and transformations for modeling soil carbon in the new century. *Biogeochemistry*, *137*(1–2), 51–71. https://doi.org/10.1007/s10533-017-0409-7

Ahrens, B., Braakhekke, M. C., Guggenberger, G., Schrumpf, M., & Reichstein, M. (2015). Contribution of sorption, DOC transport and microbial interactions to the 14C age of a soil organic carbon profile: Insights from a calibrated process model. *Soil Biology and Biochemistry*, *88*, 390–402. https://doi.org/10.1016/j.soilbio.2015.06.008

Ahrens, B., Guggenberger, G., Rethemeyer, J., John, S., Marschner, B., Heinze, S., et al. (2020). Combination of energy limitation and sorption capacity explains 14C depth gradients. *Soil Biology and Biochemistry*, *148*, 1–15. https://doi.org/10.1016/j.soilbio.2020.107912

Allison, S. D. (2012). A trait-based approach for modelling microbial litter decomposition. *Ecology Letters*, *15*(9), 1058–1070. https://doi.org/10.1111/j.1461-0248.2012.01807.x

Allison, S. D., Wallenstein, M. D., & Bradford, M. A. (2010). Soil-carbon response to warming dependent on microbial physiology. *Nature Geoscience*, *3*(5), 336–340. https://doi.org/10.1038/ngeo846

Alster, C. J., Baas, P., Wallenstein, M. D., Johnson, N. G., & von Fischer, J. C. (2016). Temperature sensitivity as a microbial trait using parameters from macromolecular rate theory. *Frontiers in Microbiology*, *7*. https://doi.org/10.3389/fmicb.2016.01821

Alster, C. J., von Fischer, J. C., Allison, S. D., & Treseder, K. K. (2020). Embracing a new paradigm for temperature sensitivity of soil microbes. *Global Change Biology*, *00*, 1–9. https://doi.org/10.1111/gcb.15053

Alster, C. J., Weller, Z. D., & von Fischer, J. C. (2018). A meta-analysis of temperature sensitivity as a microbial trait. *Global Change Biology*, *24*(9), 4211–4224. https://doi.org/10.1111/gcb.14342

Arcus, V. L., Prentice, E. J., Hobbs, J. K., Mulholland, A. J., Van der Kamp, M. W., Pudney, C. R., et al. (2016). On the temperature dependence of enzyme-catalyzed rates. *Biochemistry*, *55*(12), 1681–1688. https://doi.org/10.1021/acs.biochem.5b01094

Arndal, M. F., Tolver, A., Larsen, K. S., Beier, C., & Schmidt, I. K. (2018). Fine root growth and vertical distribution in response to elevated CO2, warming and drought in a mixed Heathland–Grassland. *Ecosystems*, *21*(1), 15–30. https://doi.org/10.1007/s10021-017-0131-2

Bååth, E. (2018). Temperature sensitivity of soil microbial activity modeled by the square root equation as a unifying model to differentiate between direct temperature effects and microbial community adaptation. *Global Change Biology*, *24*(7), 2850–2861. https://doi.org/10.1111/gcb.14285

Bárcenas-Moreno, G., Gómez-Brandón, M., Rousk, J., & Bååth, E. (2009). Adaptation of soil microbial communities to temperature: Comparison of fungi and bacteria in a laboratory experiment. *Global Change Biology*, *15*(12), 2950–2957. https://doi.org/10.1111/j.1365-2486.2009.01882.x

Boose, E., & Gould, E. (2004). *Shaler meteorological station at Harvard forest 1964-2002. Harvard forest data archive: HF000 (v.17)*. Environmental Data Initiative. https://doi.org/10.6073/pasta/213335f5daa17222a738c105b9fa60c4

Bradford, M. A. (2013). Thermal adaptation of decomposer communities in warming soils. *Frontiers in Microbiology*, *4*, 1–16. https://doi.org/10.3389/fmicb.2013.00333

Bradford, M. A., Davies, C. A., Frey, S. D., Maddox, T. R., Melillo, J. M., Mohan, J. E., et al. (2008). Thermal adaptation of soil microbial respiration to elevated temperature. *Ecology Letters*, *11*(12), 1316–1327. https://doi.org/10.1111/j.1461-0248.2008.01251.x

Bradford, M. A., McCulley, R. L., Crowther, T. W., Oldfield, E. E., Wood, S. A., & Fierer, N. (2019). Cross-biome patterns in soil microbial respiration predictable from evolutionary theory on thermal adaptation. *Nature Ecology & Evolution*, *3*(2), 223–231. https://doi.org/10.1038/s41559-018-0771-4

Bradford, M. A., Wallenstein, M. D., Allison, S. D., Treseder, K. K., Frey, S. D., Watts, B. W., et al. (2009). Decreased mass specific respiration under experimental warming is robust to the microbial biomass method employed. *Ecology Letters*, *12*(7), E15–E18. https://doi.org/10.1111/j.1461-0248.2009.01332.x

Bradford, M. A., Watts, B. W., & Davies, C. A. (2010). Thermal adaptation of heterotrophic soil respiration in laboratory microcosms. *Global Change Biology*, *16*(5), 1576–1588. https://doi.org/10.1111/j.1365-2486.2009.02040.x

Bradford, M. A., Wieder, W. R., Bonan, G. B., Fierer, N., Raymond, P. A., & Crowther, T. W. (2016). Managing uncertainty in soil carbon feedbacks to climate change. *Nature Climate Change*, *6*(8), 751–758. https://doi.org/10.1038/nclimate3071

Brzostek, E. R., Fisher, J. B., & Phillips, R. P. (2014). Modeling the carbon cost of plant nitrogen acquisition: Mycorrhizal trade-offs and multipath resistance uptake improve predictions of retranslocation. *Journal of Geophysical Research: Biogeosciences*, *119*(8), 1684–1697. https://doi.org/10.1002/2014JG002660

Butler, S. M., Melillo, J. M., Johnson, J. E., Mohan, J., Steudler, P. A., Lux, H., et al. (2012). Soil warming alters nitrogen cycling in a new England forest: Implications for ecosystem function and structure. *Oecologia*, *168*(3), 819–828. https://doi.org/10.1007/s00442-011-2133-7

Contosta, A. R., Frey, S. D., & Cooper, A. B. (2011). Seasonal dynamics of soil respiration and N mineralization in chronically warmed and fertilized soils. *Ecosphere*, *2*(3), art36. https://doi.org/10.1890/ES10-00133.1

Dacal, M., Bradford, M. A., Plaza, C., Maestre, F. T., & García-Palacios, P. (2019). Soil microbial respiration adapts to ambient temperature in global drylands. *Nature Ecology & Evolution*, *3*(2), 232–238. https://doi.org/10.1038/s41559-018-0770-5

DeAngelis, K. M., Melillo, J. M., & Pold, G. (2017). Effects of warming on soil biogeochemistry at Harvard forest 2014-2015. Harvard Forest Data Archive: HF303.

DeAngelis, K. M., Pold, G., Topcuoglu, B. D., van Diepen, L. T. A., Varney, R. M., Blanchard, J. L., et al. (2015). Long-term forest soil warming alters microbial communities in temperate forest soils. *Frontiers in Microbiology*, *6*, 1–13. https://doi.org/10.3389/fmicb.2015.00104

Dwivedi, D., Riley, W. J., Torn, M. S., Spycher, N., Maggi, F., & Tang, J. Y. (2017). Mineral properties, microbes, transport, and plant-input profiles control vertical distribution and age of soil carbon stocks. *Soil Biology and Biochemistry*, *107*, 244–259. https://doi.org/10.1016/j.soilbio.2016.12.019

Eliasson, P. E., McMurtrie, R. E., Pepper, D. A., Stromgren, M., Linder, S., & Agren, G. I. (2005). The response of heterotrophic CO2 flux to soil warming. *Global Change Biology*, *11*(1), 167–181. https://doi.org/10.1111/j.1365-2486.2004.00878.x

Eyring, H. (1935). The activated complex in chemical reactions. *The Journal of Chemical Physics*, *3*(2), 107–115. https://doi.org/10.1063/1.1749604

Finzi, A., Giasson, M., & Barker Plotkin, A. (2019). Carbon budget at the Harvard forest 1992-2015. In *Harvard forest data archive: HF324 (v.4)*. Environmental Data Initiative. https://doi.org/10.6073/pasta/62252606959b16dc17bad54be5e6300e

Finzi, A., Giasson, M., & Barker Plotkin, A. (2021). *Carbon budget at the Harvard forest 1992-2015 ver 4*. Environmental Data Initiative. https://doi.org/10.6073/pasta/62252606959b16dc17bad54be5e6300e

Finzi, A. C., Giasson, M.-A., Plotkin, A. A. B., Aber, J. D., Boose, E. R., Davidson, E. A., et al. (2020). Carbon budget of the Harvard forest long-term ecological research site: Pattern, process, and response to global change. *Ecological Monographs*, *90*(4), e01423. https://doi.org/10.1002/ecm.1423

Frey, S. D., Drijber, R., Smith, H., & Melillo, J. (2008). Microbial biomass, functional capacity, and community structure after 12 years of soil warming. *Soil Biology and Biochemistry*, *40*(11), 2904–2907. https://doi.org/10.1016/j.soilbio.2008.07.020

Frey, S. D., & Melillo, J. M. (2021). Barre woods soil warming experiment at Harvard forest since 2001. *Harvard Forest Data Archive: HF018*.

Frey, S. D., & Ollinger, S. (2021). Chronic nitrogen amendment experiment at Harvard forest since 1988. Harvard forest data archive: HF008.

Friedlingstein, P., Bopp, L., Ciais, P., Dufresne, J.-L., Fairhead, L., LeTreut, H., et al. (2001). Positive feedback between future climate change and the carbon cycle. *Geophysical Research Letters*, *28*(8), 1543–1546. https://doi.org/10.1029/2000GL012015

Friedlingstein, P., Meinshausen, M., Arora, V. K., Jones, C. D., Anav, A., Liddicoat, S. K., & Knutti, R. (2014). Uncertainties in CMIP5 climate projections due to carbon cycle feedbacks. *Journal of Climate*, *27*(2), 511–526. https://doi.org/10.1175/JCLI-D-12-00579.1

Gaudinski, J. B., Trumbore, S. E., Davidson, E. A., & Zheng, S. (2000). Soil carbon cycling in a temperate forest: Radiocarbon-based estimates of residence times, sequestration rates and partitioning of fluxes. *Biogeochemistry*, *51*(1), 33–69. https://doi.org/10.1023/A:1006301010014

Georgiou, K., Abramoff, R. Z., Harte, J., Riley, W. J., & Torn, M. S. (2017). Microbial community-level regulation explains soil carbon responses to long-term litter manipulations. *Nature Communications*, *8*(1), 1223. https://doi.org/10.1038/s41467-017-01116-z

Grant, R. F. (2014). Nitrogen mineralization drives the response of forest productivity to soil warming: Modelling in ecosys vs. measurements from the Harvard soil heating experiment. *Ecological Modelling*, *288*, 38–46. https://doi.org/10.1016/j.ecolmodel.2014.05.015

Grant, R. F., Mekonnen, Z. A., Riley, W. J., Arora, B., & Torn, M. S. (2017). Mathematical modelling of Arctic polygonal tundra with Ecosys: 2. Microtopography determines how CO_2 and CH_4 exchange responds to changes in temperature and precipitation. *Journal of Geophysical Research: Biogeosciences*, *122*(12), 3174–3187. https://doi.org/10.1002/2017JG004037

Guo, X., Gao, Q., Yuan, M., Wang, G., Zhou, X., Feng, J., et al. (2020). Gene-informed decomposition model predicts lower soil carbon loss due to persistent microbial adaptation to warming. *Nature Communications*, *11*(1), 4897. https://doi.org/10.1038/s41467-020-18706-z

Hagerty, S. B., van Groenigen, K. J., Allison, S. D., Hungate, B. A., Schwartz, E., Koch, G. W., et al. (2014). Accelerated microbial turnover but constant growth efficiency with warming in soil. *Nature Climate Change*, *4*(10), 903–906. https://doi.org/10.1038/nclimate2361

Hartley, I. P., Heinemeyer, A., & Ineson, P. (2007). Effects of three years of soil warming and shading on the rate of soil respiration: Substrate availability and not thermal acclimation mediates observed response. *Global Change Biology*, *13*(8), 1761–1770. https://doi.org/10.1111/j.1365-2486.2007.01373.x

Hartley, I. P., Hopkins, D. W., Garnett, M. H., Sommerkorn, M., & Wookey, P. A. (2009). No evidence for compensatory thermal adaptation of soil microbial respiration in the study of Bradford et al. (2008). *Ecology Letters*, *12*(7), 14–16. https://doi.org/10.1111/j.1461-0248.2009.01300.x

Hobbs, J. K., Jiao, W., Easter, A. D., Parker, E. J., Schipper, L. A., & Arcus, V. L. (2013). Change in heat capacity for enzyme catalysis determines temperature dependence of enzyme catalyzed rates. *ACS Chemical Biology*, *8*(11), 2388–2393. https://doi.org/10.1021/cb4005029

IPCC. (2023). Summary for policymakers. In H. Lee & J. Romero (Eds.), *Climate change 2023: Synthesis report. Contribution of working Groups I, II and III to the Sixth assessment report of the Intergovernmental Panel on climate change [Core Writing Team]* (pp. 1–34). IPCC. https://doi.org/10.59327/IPCC/AR6-9789291691647.001

Jarvis, P., & Linder, S. (2000). Constraints to growth of boreal forests. *Nature*, *405*(6789), 904–905. https://doi.org/10.1038/35016154

Jones, C., Robertson, E., Arora, V., Friedlingstein, P., Shevliakova, E., Bopp, L., et al. (2013). Twenty-first-Century compatible CO2 emissions and airborne fraction simulated by CMIP5 Earth system models under four representative concentration pathways. *Journal of Climate*, *26*(13), 4398–4413. https://doi.org/10.1175/JCLI-D-12-00554.1

Kirschbaum, M. U. F. (2000). Will changes in soil organic carbon act as a positive or negative feedback on global warming? *Biogeochemistry*, *48*(1), 21–51. https://doi.org/10.1023/A:1006238902976

Kirschbaum, M. U. F. (2004). Soil respiration under prolonged soil warming: Are rate reductions caused by acclimation or substrate loss? *Global Change Biology*, *10*(11), 1870–1877. https://doi.org/10.1111/j.1365-2486.2004.00852.x

Kleber, M., & Lehmann, J. (2019). Humic substances extracted by Alkali are invalid proxies for the dynamics and functions of organic matter in terrestrial and aquatic ecosystems. *Journal of Environmental Quality*, *48*(2), 207–216. https://doi.org/10.2134/jeq2019.01.0036

Knorr, M. A., Contosta, A. R., Morrison, E. W., Muratore, T. J., Anthony, M. A., Stoica, I., et al. (2024). Unexpected sustained soil carbon flux in response to simultaneous warming and nitrogen enrichment compared with single factors alone. *Nature Ecology & Evolution*. https://doi.org/10.1038/s41559-024-02546-x

Knorr, W., Prentice, I. C., House, J. I., & Holland, E. A. (2005). Long-term sensitivity of soil carbon turnover to warming. *Nature*, *433*(7023), 298–301. https://doi.org/10.1038/nature03226

Kooijman, S. A. L. M., Sousa, T., Pecquerie, L., van der Meer, J., & Jager, T. (2008). From food-dependent statistics to metabolic parameters, a practical guide to the use of dynamic energy budget theory. *Biological Reviews*, *83*(4), 533–552. https://doi.org/10.1111/j.1469-185X.2008.00053.x

Lehmann, J., & Kleber, M. (2015). The contentious nature of soil organic matter. *Nature*, *528*(7580), 60–68. https://doi.org/10.1038/nature16069

Li, J., Wang, G., Mayes, M. A., Allison, S. D., Frey, S. D., Shi, Z., et al. (2018). Reduced carbon use efficiency and increased microbial turnover with soil warming. *Global Change Biology*, *25*(gcb), 14517–14910. https://doi.org/10.1111/gcb.14517

Li, Y., Lv, W., Jiang, L., Zhang, L., Wang, S., Wang, Q., et al. (2019). Microbial community responses reduce soil carbon loss in Tibetan alpine grasslands under short-term warming. *Global Change Biology*, *25*(10), 3438–3449. https://doi.org/10.1111/gcb.14734

Liu, X. J. A., Pold, G., Domeignoz-Horta, L. A., Geyer, K. M., Caris, H., Nicolson, H., et al. (2021). Soil aggregate-mediated microbial responses to long-term warming. *Soil Biology and Biochemistry*, *152*, 108055. https://doi.org/10.1016/j.soilbio.2020.108055

Magill, A. H., Aber, J. D., Currie, W. S., Nadelhoffer, K. J., Martin, M. E., McDowell, W. H., et al. (2004). Ecosystem response to 15 years of chronic nitrogen additions at the Harvard Forest LTER, Massachusetts, USA. *Forest Ecology and Management*, *196*(1), 7–28. https://doi.org/10.1016/j.foreco.2004.03.033

McFarlane, K. J., Torn, M. S., Hanson, P. J., Porras, R. C., Swanston, C. W., Callaham, M. A., & Guilderson, T. P. (2013). Comparison of soil organic matter dynamics at five temperate deciduous forests with physical fractionation and radiocarbon measurements. *Biogeochemistry*, *112*(1–3), 457–476. https://doi.org/10.1007/s10533-012-9740-1

Mekonnen, Z. A., Riley, W. J., & Grant, R. F. (2018). 21st century tundra shrubification could enhance net carbon uptake of North America Arctic tundra under an RCP8.5 climate trajectory. *Environmental Research Letters*, *13*(5), 054029. https://doi.org/10.1088/1748-9326/aabf28

Melillo, J. M., Butler, S., Johnson, J., Mohan, J., Steudler, P., Lux, H., et al. (2011). Soil warming, carbon-nitrogen interactions, and forest carbon budgets. *Proceedings of the National Academy of Sciences*, *108*(23), 9508–9512. https://doi.org/10.1073/pnas.1018189108

Melillo, J. M., Frey, S. D., DeAngelis, K. M., Werner, W. J., Bernard, M. J., Bowles, F. P., et al. (2017). Long-term pattern and magnitude of soil carbon feedback to the climate system in a warming world. *Science*, *358*(6359), 101–105. https://doi.org/10.1126/science.aan2874

Melillo, J. M., Steudler, P. A., Aber, J. D., Newkirk, K., Lux, H., Bowles, F. P., et al. (2002). Soil warming and carbon-cycle feedbacks to the climate system. *Science*, *298*(5601), 2173–2176. https://doi.org/10.1126/science.1074153

Morrison, E. W., Pringle, A., van Diepen, L. T. A., Grandy, A. S., Melillo, J. M., & Frey, S. D. (2019). Warming alters fungal communities and litter chemistry with implications for soil carbon stocks. *Soil Biology and Biochemistry*, *132*, 120–130. https://doi.org/10.1016/j.soilbio.2019.02.005

Munger, W., & Wofsy, S. (2021). Biomass inventories at Harvard forest EMS tower since 1993. *Harvard Forest Data Archive: HF069*.

Nottingham, A. T., Bååth, E., Reischke, S., Salinas, N., & Meir, P. (2019). Adaptation of soil microbial growth to temperature: Using a tropical elevation gradient to predict future changes. *Global Change Biology*, *25*(3), 827–838. https://doi.org/10.1111/gcb.14502

Oechel, W. C., Vourlitis, G. L., Hastings, S. J., Zulueta, R. C., Hinzman, L., & Kane, D. (2000). Acclimation of ecosystem CO 2 exchange in the Alaskan Arctic in response to decadal climate warming. *Nature*, *406*(6799), 978–981. https://doi.org/10.1038/35023137

Oliverio, A. M., Bradford, M. A., & Fierer, N. (2017). Identifying the microbial taxa that consistently respond to soil warming across time and space. *Global Change Biology*, *23*(5), 2117–2129. https://doi.org/10.1111/gcb.13557

Parton, W. J., Schimel, D. S., Cole, C. V., & Ojima, D. S. (1987). Analysis of factors controlling soil organic matter levels in Great Plains grasslands. *Soil Science Society of America Journal*, *51*(5), 1173–1179. https://doi.org/10.2136/sssaj1987.03615995005100050015x

Pold, G., Billings, A. F., Blanchard, J. L., Burkhardt, D. B., Frey, S. D., Melillo, J. M., et al. (2016). Long-term warming alters carbohydrate degradation potential in temperate forest soils. *Applied and Environmental Microbiology*, *82*(22), 6518–6530. https://doi.org/10.1128/AEM.02012-16

Pold, G., Grandy, A. S., Melillo, J. M., & DeAngelis, K. M. (2017). Changes in substrate availability drive carbon cycle response to chronic warming. *Soil Biology and Biochemistry*, *110*, 68–78. https://doi.org/10.1016/j.soilbio.2017.03.002

Pold, G., Melillo, J. M., & DeAngelis, K. M. (2015). Two decades of warming increases diversity of a potentially lignolytic bacterial community. *Frontiers in Microbiology*, *6*. https://doi.org/10.3389/fmicb.2015.00480

Ratkowsky, D. A., Olley, J., McMeekin, T. A., & Ball, A. (1982). Relationship between temperature and growth rate of bacterial cultures. *Journal of Bacteriology*, *149*(1), 1–5. https://doi.org/10.1128/jb.149.1.1-5.1982

Riley, W. J., Maggi, F., Kleber, M., Torn, M. S., Tang, J. Y., Dwivedi, D., & Guerry, N. (2014). Long residence times of rapidly decomposable soil organic matter: Application of a multi-phase, multi-component, and vertically resolved model (BAMS1) to soil carbon dynamics. *Geoscientific Model Development*, *7*(4), 1335–1355. https://doi.org/10.5194/gmd-7-1335-2014

Riley, W. J., Sierra, C. A., Tang, J., Bouskill, N. J., Zhu, Q., & Abramoff, R. Z. (2022). Next generation soil biogeochemistry model representations: A proposed community open source model farm (BeTR-S). In Y. Yang, M. Keiluweit, N. Senesi, & B. Xing (Eds.), *Multi-scale biogeochemical processes in soil ecosystems* (1st ed., pp. 233–257). Wiley. https://doi.org/10.1002/9781119480419.ch11

Rousk, J., Frey, S. D., & Bååth, E. (2012). Temperature adaptation of bacterial communities in experimentally warmed forest soils. *Global Change Biology*, *18*(10), 3252–3258. https://doi.org/10.1111/j.1365-2486.2012.02764.x

Rustad, L., Campbell, J., Marion, G., Norby, R., Mitchell, M., Hartley, A., et al. (2001). A meta-analysis of the response of soil respiration, net nitrogen mineralization, and aboveground plant growth to experimental ecosystem warming. *Oecologia*, *126*(4), 543–562. https://doi.org/10.1007/s004420000544

Savage, K. E., Davidson, E. A., Abramoff, R. Z., Finzi, A. C., & Giasson, M.-A. (2018). Partitioning soil respiration: Quantifying the artifacts of the trenching method. *Biogeochemistry*, *140*(1), 53–63. https://doi.org/10.1007/s10533-018-0472-8

Scharlemann, J. P., Tanner, E. V., Hiederer, R., & Kapos, V. (2014). Global soil carbon: Understanding and managing the largest terrestrial carbon pool. *Carbon Management*, *5*(1), 81–91. https://doi.org/10.4155/cmt.13.77

Schimel, J. P., & Weintraub, M. N. (2003). The implications of exoenzyme activity on microbial carbon and nitrogen limitation in soil: A theoretical model. *Soil Biology and Biochemistry*, *35*(4), 549–563. https://doi.org/10.1016/S0038-0717(03)00015-4

Schipper, L. A., Hobbs, J. K., Rutledge, S., & Arcus, V. L. (2014). Thermodynamic theory explains the temperature optima of soil microbial processes and high Q10 values at low temperatures. *Global Change Biology*, *20*(11), 3578–3586. https://doi.org/10.1111/gcb.12596

Schuur, E. A. G., Druffel, E., & Trumbore, S. E. (Eds.). (2016). *Radiocarbon and climate change*. Springer International Publishing. https://doi.org/10.1007/978-3-319-25643-6

Sierra, C. A., Malghani, S., & Müller, M. (2015). Model structure and parameter identification of soil organic matter models. *Soil Biology and Biochemistry*, *90*, 197–203. https://doi.org/10.1016/j.soilbio.2015.08.012

Song, J., Wan, S., Piao, S., Knapp, A. K., Classen, A. T., Vicca, S., et al. (2019). A meta-analysis of 1,119 manipulative experiments on terrestrial carbon-cycling responses to global change. *Nature Ecology & Evolution*, *3*(9), 1309–1320. https://doi.org/10.1038/s41559-019-0958-3

Sulman, B. N., Moore, J. A. M., Abramoff, R. Z., Averill, C., Kivlin, S., Georgiou, K., et al. (2018). Multiple models and experiments underscore large uncertainty in soil carbon dynamics. *Biogeochemistry*, *141*(2), 109–123. https://doi.org/10.1007/s10533-018-0509-z

Tang, J. Y., & Riley, W. J. (2013). A total quasi-steady-state formulation of substrate uptake kinetics in complex networks and an example application to microbial litter decomposition. *Biogeosciences*, *10*(12), 8329–8351. https://doi.org/10.5194/bg-10-8329-2013

Tang, J. Y., & Riley, W. J. (2015). Weaker soil carbon–climate feedbacks resulting from microbial and abiotic interactions. *Nature Climate Change*, *5*(1), 56–60. https://doi.org/10.1038/nclimate2438

Tang, J. Y., & Riley, W. J. (2024). A chemical kinetics theory for interpreting the non-monotonic temperature dependence of enzymatic reactions. *Biogeosciences*, *21*(5), 1061–1070. https://doi.org/10.5194/bg-21-1061-2024

Todd-Brown, K. E. O., Randerson, J. T., Hopkins, F., Arora, V., Hajima, T., Jones, C., et al. (2014). Changes in soil organic carbon storage predicted by Earth system models during the 21st century. *Biogeosciences*, *11*(8), 2341–2356. https://doi.org/10.5194/bg-11-2341-2014

Van de Broek, M., & Tang, J. (2024). ReSOM-Van-de-Broek-et-al.-JGR-Biogeosciences: ReSOM [Software]. *Zenodo*. https://doi.org/10.5281/zenodo.13740358

Vicca, S., Fivez, L., Kockelbergh, F., Pelt, D. V., Segers, J. J. R., Meire, P., et al. (2009). No signs of thermal acclimation of heterotrophic respiration from peat soils exposed to different water levels. *Soil Biology and Biochemistry*, *41*(9), 2014–2016. https://doi.org/10.1016/j.soilbio.2009.07.007

Walker, T. W. N., Kaiser, C., Strasser, F., Herbold, C. W., Leblans, N. I. W., Woebken, D., et al. (2018). Microbial temperature sensitivity and biomass change explain soil carbon loss with warming. *Nature Climate Change*, *8*(10), 885–889. https://doi.org/10.1038/s41558-018-0259-x

Wieder, W. R., Bonan, G. B., & Allison, S. D. (2013). Global soil carbon projections are improved by modelling microbial processes. *Nature Climate Change*, *3*(10), 909–912. https://doi.org/10.1038/nclimate1951

Wieder, W. R., Grandy, A. S., Kallenbach, C. M., & Bonan, G. B. (2014). Integrating microbial physiology and physio-chemical principles in soils with the MIcrobial-MIneral Carbon Stabilization (MIMICS) model. *Biogeosciences*, *11*(14), 3899–3917. https://doi.org/10.5194/bg-11-3899-2014

Wieder, W. R., Hartman, M. D., Sulman, B. N., Wang, Y.-P., Koven, C. D., & Bonan, G. B. (2018). Carbon cycle confidence and uncertainty: Exploring variation among soil biogeochemical models. *Global Change Biology*, *24*(4), 1563–1579. https://doi.org/10.1111/gcb.13979

Wu, Z., Dijkstra, P., Koch, G. W., Peñuelas, J., & Hungate, B. A. (2011). Responses of terrestrial ecosystems to temperature and precipitation change: A meta-analysis of experimental manipulation. *Global Change Biology*, *17*(2), 927–942. https://doi.org/10.1111/j.1365-2486.2010.02302.x

Yan, Z., Bond-Lamberty, B., Todd-Brown, K. E., Bailey, V. L., Li, S., Liu, C., & Liu, C. (2018). A moisture function of soil heterotrophic respiration that incorporates microscale processes. *Nature Communications*, *9*, 1–10. https://doi.org/10.1038/s41467-018-04971-6

Zhang, H., Goll, D. S., Wang, Y.-P., Ciais, P., Wieder, W. R., Abramoff, R. Z., et al. (2020). Microbial dynamics and soil physicochemical properties explain large-scale variations in soil organic carbon. *Global Change Biology*, *26*(4), 2668–2685. https://doi.org/10.1111/gcb.14994

Zhou, J., Xue, K., Xie, J., Deng, Y., Wu, L., Cheng, X., et al. (2012). Microbial mediation of carbon-cycle feedbacks to climate warming. *Nature Climate Change*, *2*(2), 106–110. https://doi.org/10.1038/nclimate1331